ABSTRACT

SWAMINATHAN, VINAY SHANKAR. Mechanics of a mosquito bite. (Under the direction of Dr. M K Ramasubramanian.)

The objective of this thesis is to provide a fundamental understading of the process of a mosquito bite. Mosquito fascicle, which is the part of the mosquito used for penetrating the skin and drawing blood, is 2mm long and 30 μm in diameter. A needle of this size to be able to penetrate a tough membrane like the human skin needs some kind of stabilization phenomena with which buckling failure can be prevented. By studying high speed video of the process and Scanning Electron Microscope images of the fascicle, a stability mechanism is observed which increases the critical buckling load of the fascicle and prevents failure. This stability mechanism is explained by using the theory of non-conservative force and Beck's column theory. To further support the argument of non-conservative forces, Finite element models of the skin penetration process is built. Since there is no published data on the properties of the fascicle, mechanical tests are conducted to get stress strain data of the fascicle to build the material model used in finite element analysis. The finite element simulations support this concept where the fascicle can only penetrate the skin with the application of non conservative forces.

Mechanics of a Mosquito Bite

by

Vinay S Swaminathan

A thesis submitted to the Graduate Faculty of

North Carolina State University

In partial fulfillment of the

Requirements for the degree of

Master of Science

In

Mechanical Engineering

Raleigh, NC

2006

Approved by:

Dr K J Peters

Dr C S Apperson

Dr M K Ramasubramanian

(Chair of advisory committee)

Dedicated to the strength of my mother and the memory of my father

BIOGRAPHY

Vinay S Swaminathan was born on the 16th day of June, 1981 in an obscure little town called Gelsenkirchen in Germany. After returning to India, and completing his Bachelors in Engineering from University of Madras, The author joined North Carolina State University in the fall of 2003.

ACKNOWLEDGMENTS

First and foremost I would like to thank my faith in god for giving me the hope in times of despair not only during the course of this project but throughout my life. My mother has played the most important role in my life. Without her my life would not be at this present juncture. I thank her for her strength, support and love. I would also like to express my profound gratitude to Dr. Ramasubramanian for giving me the opportunity to work on this project and providing me with the guidance to complete it and helping me find the right direction when it seemed that there were none. I hope I am able to justify his belief in this project and me. I also would like to thank Dr. Apperson for his support during the course of the project and knowledge in the field of mosquitoes, which was a complete unknown before this project commenced and Dr. Peters for evaluating the project as a committee member. My heartfelt gratitude extends to my sister and brother in law who never made me feel homesick in a new country and have been my pillars of support over the past 2 years. None of this would have been possible without the guidance of the above-mentioned people and without the support of my research group. No life is complete without friends and I like to thank all the people I have had an opportunity to know, for bearing through my quirks during some tough times. And finally I would like to thank a special person called Ramya for her undying support, confidence, patience, and love and for making me look forward to the future with anticipation.

TABLE OF CONTENTS

List of Figures ..... **vi**

List of Tables ..... **vii**

Chapter 1 ..... **1**

Introduction: **1**

1.1 Background 1
1.2 Theory of Failure in Microneedles 2
1.3 Microneedle Fabrication 3
1.4 Blood feeding in mosquitoes. 5
1.5 Structure of the fascicle 6

Chapter 2 ..... **8**

Physical characterization of a mosquito biting parts **8**

2.1 Scanning electron Microscope imaging 8
2.2 High speed video imaging of the mosquito feeding process 14
2.2.1 Observation and initial conclusions *14*
2.3. Application of Non-Conservative force 18

Chapter 3 ..... **21**

Stability Mechanisms **21**

3.1. Theory of elastic Foundation 21
3.2 Theory of non-conservative force 23
3.3. Methods of Application: 28

CHAPTER 4 ..... **30**

Mechanical testing of Fascicle **30**

4.1 Introduction 30
4.2 Experimental protocol 30
4.2.1 Sample Preparation *30*
4.3 Test Set up 33
4.3.1 Challenges in Testing *34*
4.4 Results and Conclusions. 36
4.4.1 Theory of Hyperelasticity [21] *38*

Chapter 5 ..... **41**

Finite Element Analysis **41**

5.1. Introduction 41
5.2. Skin Model 42
5.3. Contact Model 44
5.4. Element Formulation 45
5.5. Results 46

Chapter 6 ..... **53**

Conclusion: **53**

List of References **54**

List of Figures

Figure 1:[5] Concept of a blood monitoring device 2
Figure 2: [9] Machined Microneedle 4
Figure 3:SEM image of the mosquito showing various parts 6
Figure 4:Female fascicle showing reinforcement at the tip 9
Figure 5:. Male fascicle tip 10
Figure 6:SEM image of fascicle showing surface detail 11
Figure 7: Cross Sectional sketch of the fascicle 13
Figure 8:Sketch of the fascicle showing the dimensions in mm. 13
Figure 9:This still image shows the probing process during feeding. 15
Figure 10: This image shows that the large impulsive force applied during the probing process is partly due to forward motion of the whole body applied by lifting and pushing of the legs 15
Figure 13: A beck's Column 24
Figure 14: Plot of equation [3] 27
Figure 15: Solution to Beck's Column 28
Figure 16: Sample Loading on a Paper Strip 32
Figure 17: Enduratec Load Frame 33
Figure 18: DAQ Set up 34
Figure 19: Stress Strain Curve for Fascicle 37
Figure 20: Hyperelastic curve fit for Fascicle Data 38
Figure 21: Layer of the skin [13] 44
Figure 22: Buckling of the needle with application of axial displacement 47
Figure 23: Load Displacement with 0.1N follower force 48
Figure 24: Contact Stress with 0.1N follower force 49
Figure 25: Load Displacement with 0.5N follower force 50
Figure 26: Contact Stress with 0.5N follower force 50
Figure 27: Load Displacement for 1N follower Force 51
Figure 28: Contact Stress with 1N follower Force 51

List of Tables

Table 1: Skin Mechanical properties [26].. 43

Chapter 1

Introduction:

1.1 Background

Development of micro needles for several biomedical applications has quickly become one of the fastest growing research fields today. With more and more people getting affected with Diabetes, micro needles present a very high potential in blood drawing for monitoring and drug delivery [1][2][3]. Patients including infants need continuous monitoring of their blood sugar levels, which so far involves a drop of blood collected from the finger tip and fed into the meter. This process is extremely painful because of the lancet used to prick the finger for the blood sample. In fact repeated use of this procedure leads to numbness in that part and patient trauma. The main idea behind the microneedle approach is that due to the small size of the needles, tissue damage will be limited and pain sensation can be reduced [4] or even completely avoided.

Over the past decade, the use of micro needles has been suggested for blood drawing to reduce this sensation of pain. Giorgio E. Gattiker, Karan V. L S. Kaler et al. [5] designed a MEMS device for blood glucose monitoring using the similar drawing technique as the blood drawing in mosquitoes. However no investigation was done on the stability of their microneedle which had dimensions of, significantly bigger than a mosquito fascicle.

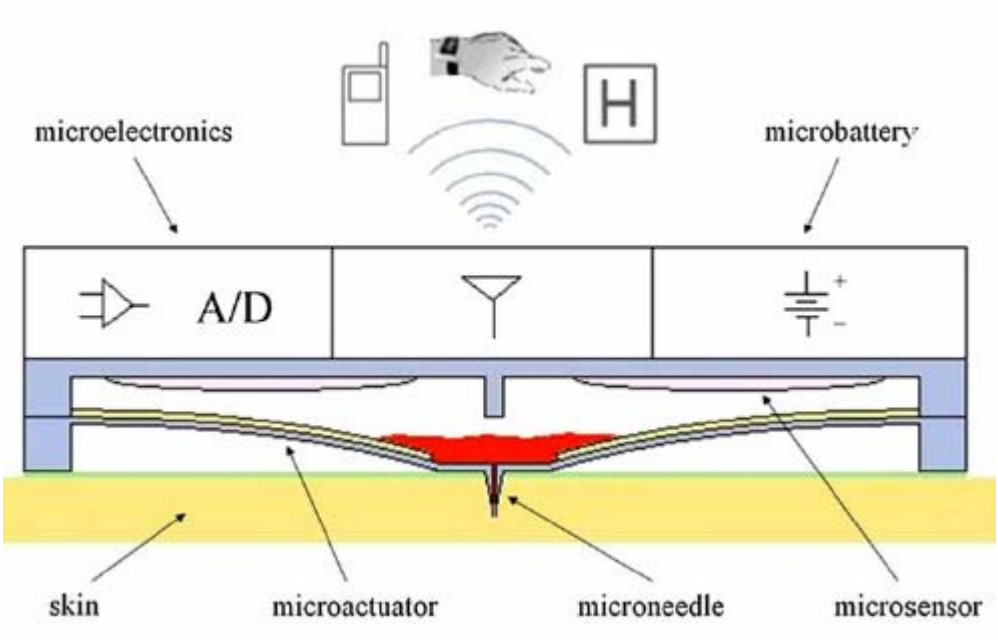

Figure 1:[5] Concept of a blood monitoring device

One of the major obstacles in this application is with the possibility of needle breakage which can lead to severe complication in patients.

1.2 Theory of Failure in Microneedles

When a microneedle penetrates a tough membrane, there is a short period of time when the needle is under high compressive stress. During this period, if the second moment of area of the microneedle is not high enough relative to its length, the microneedle will buckle. For buckling analysis of microneedles, it is necessary to determine whether the buckling will be short column buckling or long column buckling. For the Euler equation for long elastic columns of length L to be applicable the slenderness ration L/k must be greater than the critical slenderness ratio [6].

$$(l/k) = \sqrt{\frac{\pi^2 EA}{4F_{cr}}}$$

where E is the Young's modulus, A is the area and F_{cr} is the critical force that will cause short column buckling. The radius of gyration k is defined as

$$k = \sqrt{\frac{I}{A}}$$

where I is the second moment of area. Thus the critical slenderness ratio is defined as

$$(L/K)_{cr} = \sqrt{\frac{\pi^2 E}{2\sigma_y}}$$

The slenderness ratio for a typical microneedle is 114. Thus microneedles can be modeled as long columns and the Euler equation for elastic buckling can be applied.

$$F = \frac{C\pi^2 EI}{L^2}$$

Zahn et al. [7] were also able to show that shear could be another possible mode of failure, and the maximum shear force V was approximated as

$$V = \frac{\sigma_y A}{2}$$

However in their study they found this value of shear force required for failure a lot higher than the buckling force, which indicates that failure buckling modes were more likely to occur.

1.3 Microneedle Fabrication

Different materials have been used in microneedle fabrication. Polysilicone needles made of ceramics have shown good potential. However ceramic needles fail due to crack initiation and propagation.

A number of techniques have been used for producing smaller and smaller needles including using silicon fabrication [7] and microneedle [8] arrays, the latter applied to transdermal drug delivery. Gardeniers, Regina Luttge et al. [9] used micro injection molding technique to fabricate plastic needles. The advantages of plastic microneedles

are that they are easily disposable, can be melted at lower temperatures and are flexible enough to be used for intravenous catheters. However they suffer from lack of strength and easy failure and the use of plastic for needles is still under investigation.

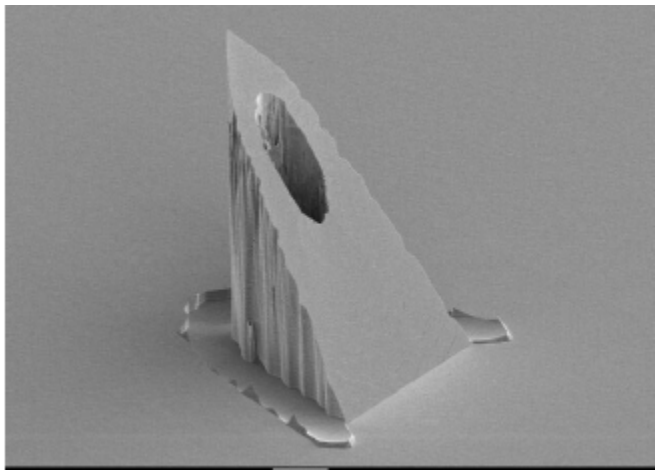

Figure 2: [9] Machined Microneedle

As mentioned earlier, Giorgio Gattiker, Karan V. L S. Kaler et al.[5] have been able to manufacture microneedles with base width of 100 μm and hole diameter of 50 μm using silicon. Silicon fabrication basically involves [8] taking a silicon wafer and growing a layer of silicon dioxide of thickness 0.7 μm and patterning it using a Deep Reactive Ion Etching (DRIE) technique. This process forms the channel with the desired width and height in the silicon wafer. The residual silicon dioxide is removed, followed by necessary cleaning of the wafers before the actual bonding takes place. The resulting wafer is fusion bonded with another silicon wafer. Once the two wafers are bonded, the top wafer is subsequently thinned down, to achieve the desired top wafer thickness. The bonded wafers are then patterned according to the desired shape and length and etched to obtain a vertical structure with high aspect ratio. Finally, patterned backside etching of the microneedle is carried out, to achieve the desired thickness.

Nature, on the other hand has been able to produce a microneedle system with 100% reliability and with a totally painless blood drawing capability. A female mosquito is able to feed on human blood without producing a sensation of pain and without any failure of its needle or fascicle. The only sensation and that of itching is produced due to the introduction of mosquito saliva which prevents clotting of the blood. The immediate aim of this project is to understand the mechanics involved in the needle insertion process, to completely characterize all aspects of this unique process and explore ways to mimic this system for a novel blood drawing device which can be used for glucose monitoring or for drug delivery in a painless manner. A female mosquito is able to draw as much as 2.5 microliters of blood which makes the system more attractive as this amount is adequate for blood glucose monitoring. Taking the concept one step further, the system could be reversed to inject insulin or other therapeutic agents back into the body when necessary in painless manner

1.4 Blood feeding in mosquitoes.

The fascicle of the *Aedes aegypti*, a common type of mosquito as observed from the scanning electron microscope pictures are 2mm long and around 30 μm in width. Therefore there are much too large to enter the capillaries (10-20 μm) located just below the epidermis in humans. They can however enter the larger arterioles and venules which are of diameter 40-60 μm in the upper and mid dermis and 100-400 μm in the deeper tissues.

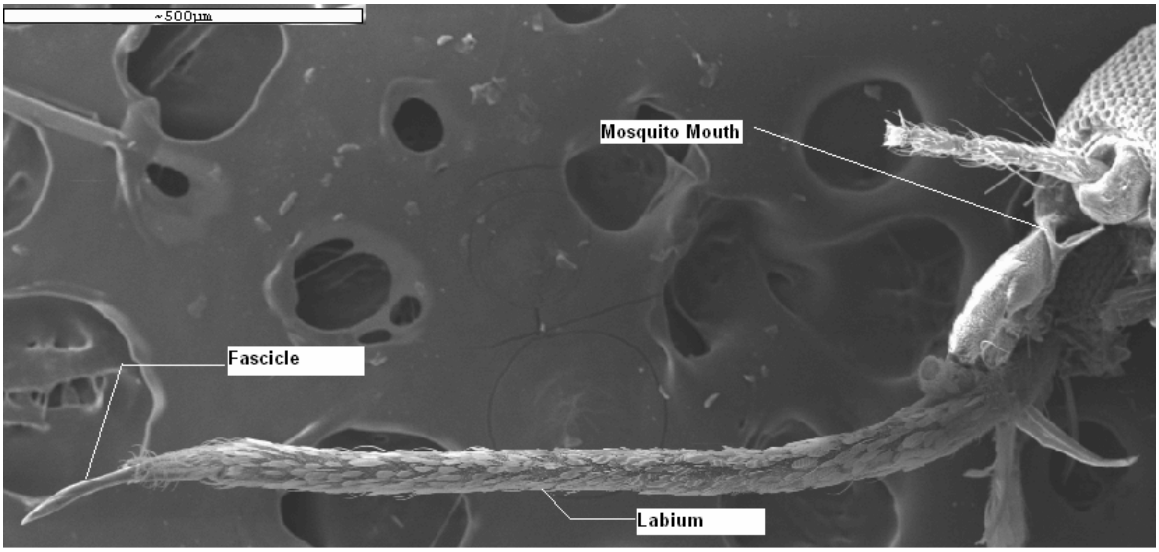

Figure 3:SEM image of the mosquito showing various parts

1.5 Structure of the fascicle

The fascicle comprises of 6 different stylets [10] which are the labrum, the paired mandibles, the hypopharynx, and the paired maxillae. In mosquitoes the labrum is the largest, stiffest and most dorsal stylet in the fascicle. The tip of the labrum curves downwards slightly and is sharpened-off ventrally like a quill pen. The mandibles are extremely thin, delicate stylets. At the base of the proboscis the mandibles occupy a lateral position in the fascicle. In Ae*. aegypti* the mandibles form the ventral closure for the salivary canal. The hypopharynx is a delicate flat unpaired stylet with a thickening along its midline which contains the salivary canal. The Maxillae are the principle piercing organs, are highly modified, each consisting of an internal rod, a stylet, a pal panda complex musculature. Near the base of the proboscis the paired maxillary stylets are lateral in location but over most of the length of the proboscis they lie side by side. The sclerotized tips of the maxillary stylets are sharply tapered and in most species their curved outer edges bear backward pointing teeth, and in some species the inner edges bear a few forward pointing teeth. The outer edges of the mandibular and the maxillary stylets interlock with the lateral grooves of the labrum. Because of the strength and

curved form of the maxillary stylets it has been suggested that it is the interlocking of the maxillary stylets and the labrum that holds the several stylets in the fascicle together [11] [12] and [13].

It is believed that it is the movements of the maxillae which are responsible for penetration of the fascicle, with the maxillary teeth acting as the grappling hooks. The movement of the right and left protractor and retractors (which are anchored to the skin by its teeth) pulls the cranium towards the skin surface and pushes the fascicle deeper into the skin.

Once the penetration is done, the tip of the fascicle has been observed to bend through almost a right angle. There is a very limited sideways movement. Mellink et al. [14] were alone in considering that the fascicle is uniformly stiff and inflexible, that it only bends passively and in response to host tissue resistance. However movement of the tip of the fascicle is ascribed to the contraction of various muscles in the labrum.

This project aims at investigating the mechanism of the skin penetration process, and understand the reasons for stability in mosquito fascicle which at very small dimension is able to penetrate the skin and withdraw blood. To be able to manufacture a needle of that dimension and integrate this needle with a blood glucose monitoring system is the long term goal of the project.

Chapter 2

Physical characterization of a mosquito biting parts

2.1 Scanning electron Microscope imaging

The first step in understanding a mosquito feeding process was to first understand the geometry of the fascicle. The questions posed were how big a fascicle is, does it have any special geometry at its tip, is there a physical reason that only the female mosquitoes feed. For this reason Scanning Electron Microscopy was used. Male and female proboscises were extracted from mosquitoes and then SEM images were obtained. Initially it was hoped that the SEM images would also reveal some surface details of the fascicle.

As predicted, the female fascicle and male fascicle had the same dimensions. However there was a stark contrast in the fascicle tip geometry.

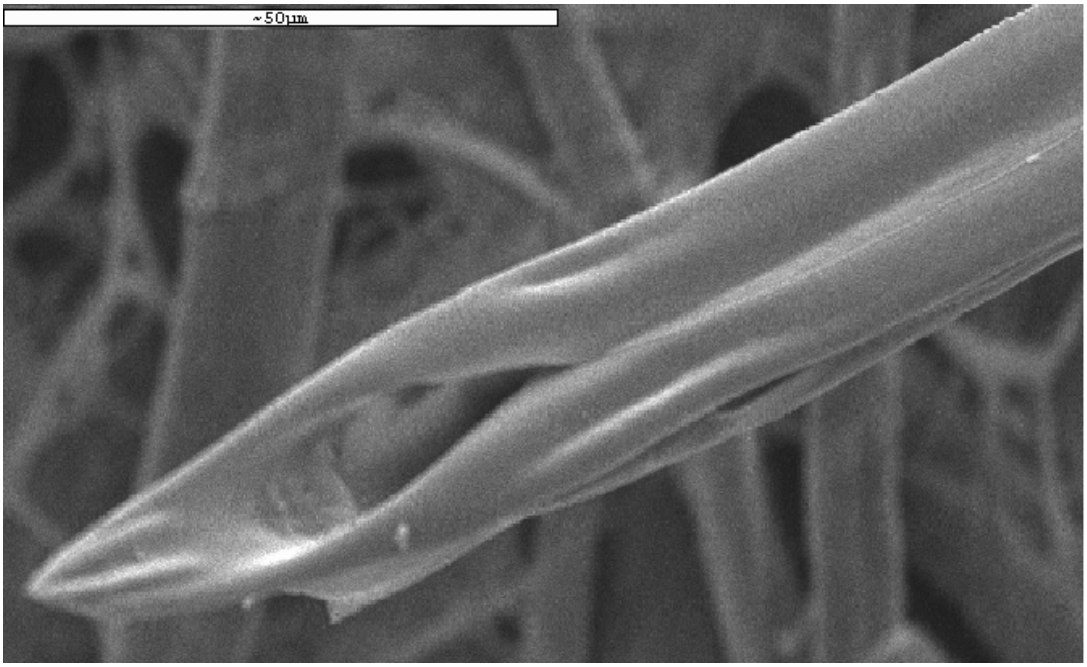

Figure 4:Female fascicle showing reinforcement at the tip

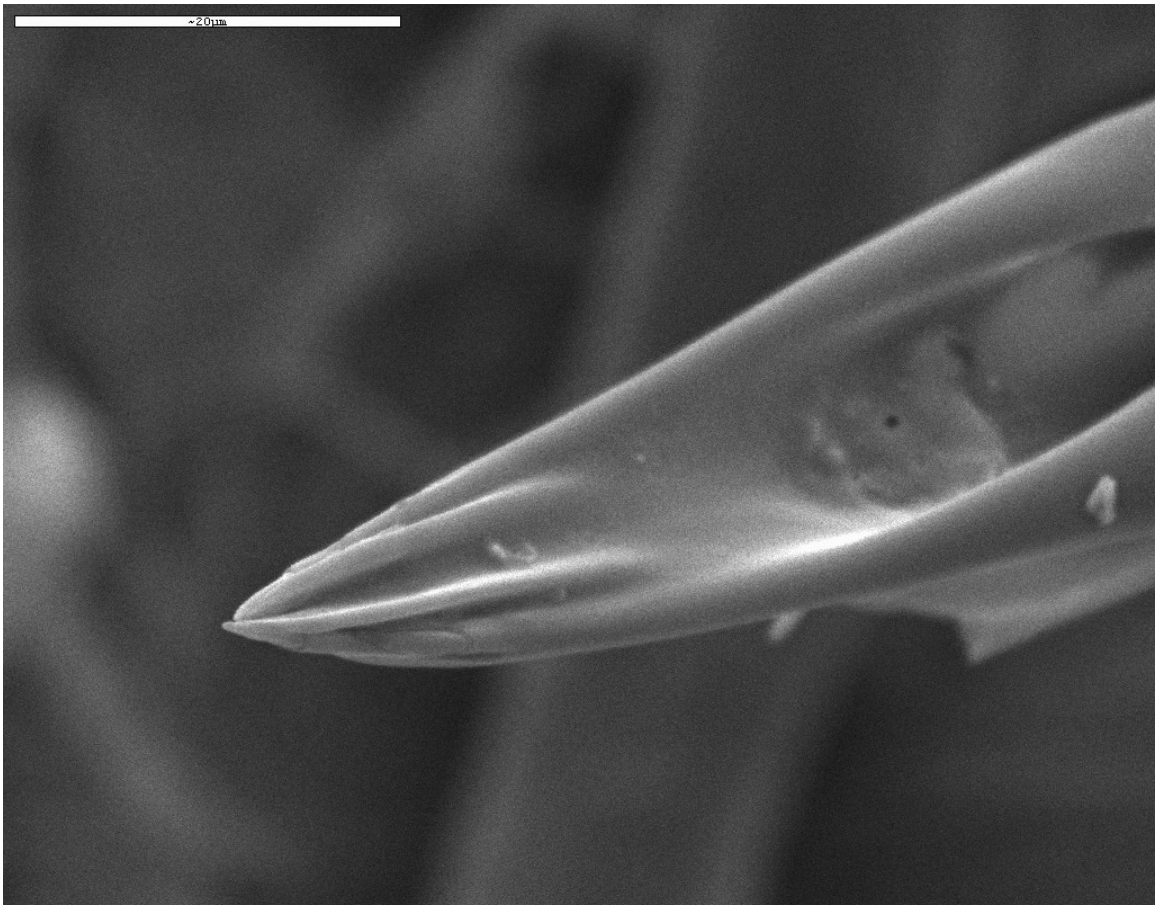

Figure 5. Close up SEM image of the female fascicle tip

The above SEM image (fig.4) clearly shows the sharp hypodermic needle like tip geometry. The close up image of the fascicle tip also shows a reinforcement structure at the tip. In contrast to this, a male fascicle (fig.5) has a blunt, scoop like geometry which it has adapted for flower nectar feeding.

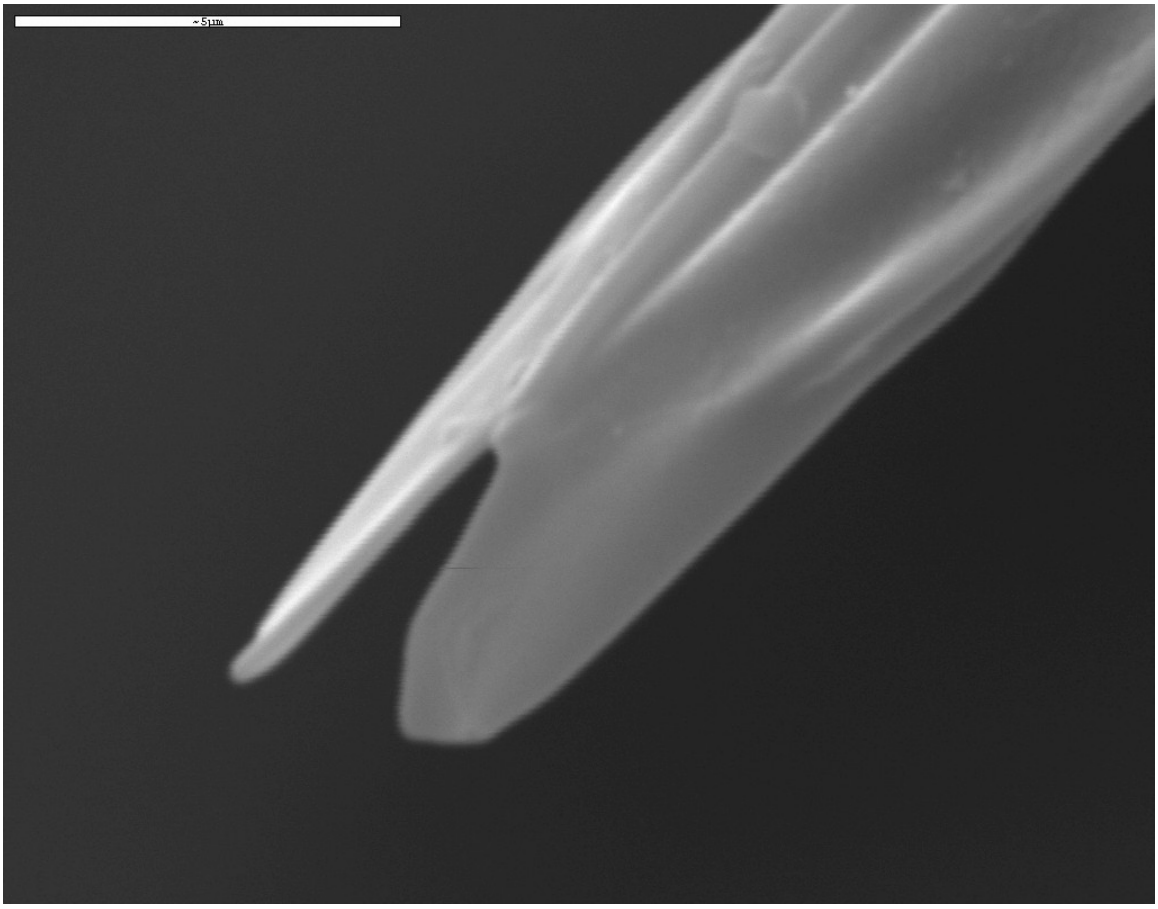

Figure 5:. Male fascicle tip

As mentioned earlier, it was also hoped that some surface detail could be obtained from the SEM images. However, due to the necessity of surface preparation to get a high resolution clear image, the SEM details didn't reveal too much of the surface characteristic as is clear from highly magnified image of the female fascicle (fig.3)

below. However not only did the SEM images help in establishing the difference in the female and male fascicles, but it helped in getting information on the fascicle geometry. On an average the mosquito fascicle was found to be 2mm in length. The fascicle is a hollow tube with an average wall thickness of 4-5 μm. At its widest, the fascicle has an outer diameter of 30 μm which tapers to form the sharp tip shown in figure above.

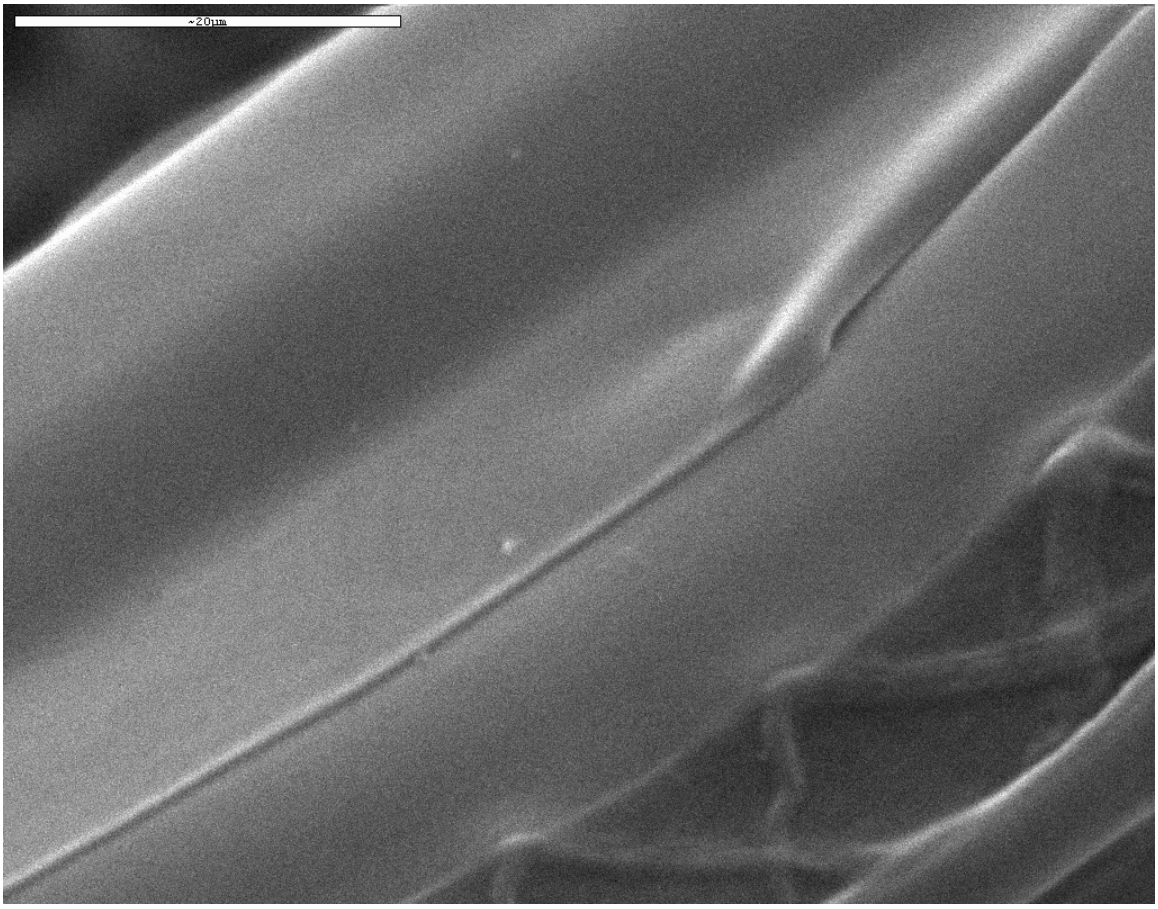

Figure 6:SEM image of fascicle showing surface detail

One of the main objectives of the project is to understand the mechanics involved in the mosquito feeding process and thus the SEM images brought forward the first challenge, to understand how the fascicle 2mm long and with an outer diameter of 30 μm at its

widest, is able to penetrate human skin and draw blood without any form of structural failure.

Thus evolves the need to understand the structural composite which forms the mosquito fascicle. The SEM images also show the smooth exterior surface of the fascicle with uniform ridges along the whole length.

A number of methods were checked for feasibility to get some form of sub structural information on a mosquito fascicle.

It has long been known that chitin is the biodegradable natural polymer based on polysaccharides, which is structural element of the exoskeleton of invertebrates such as crabs, shrimps, lobsters and all insects including mosquitoes. Chitin has a micro fibular structure. However because of the observed rigidity of the fascicle, it is apparent that some form of cross linking in the chitin fibers plays an important role.

Most chitin characterization in the past 10 or 15 years has been carried out by solid state NMR. However, for characterization of the chitin required in fascicles, we would require hundreds of fascicles which practically is a very tough task. Hence for this research study chitin was assumed to be the constitutive material of the fascicle.

Thus the SEM study helped in not only understanding the basic difference in male and female fascicle but more importantly helped in approximating the dimensions of the fascicle, the radius of the tip curvature and thickness of the fascicle, all of which were necessary in experimentation and Finite element modeling.

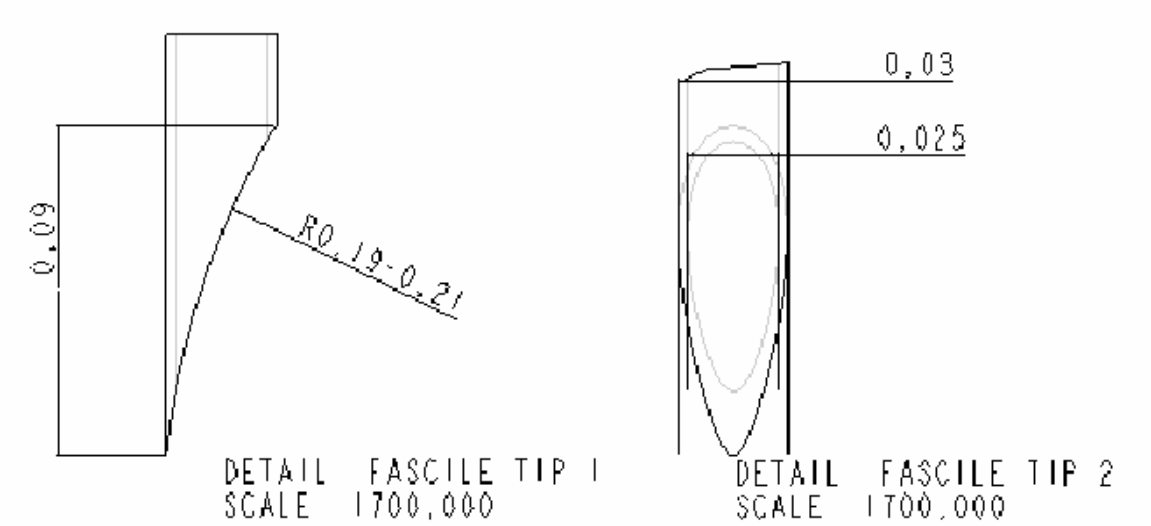

Figure 7: Cross Sectional schematic of the fascicle

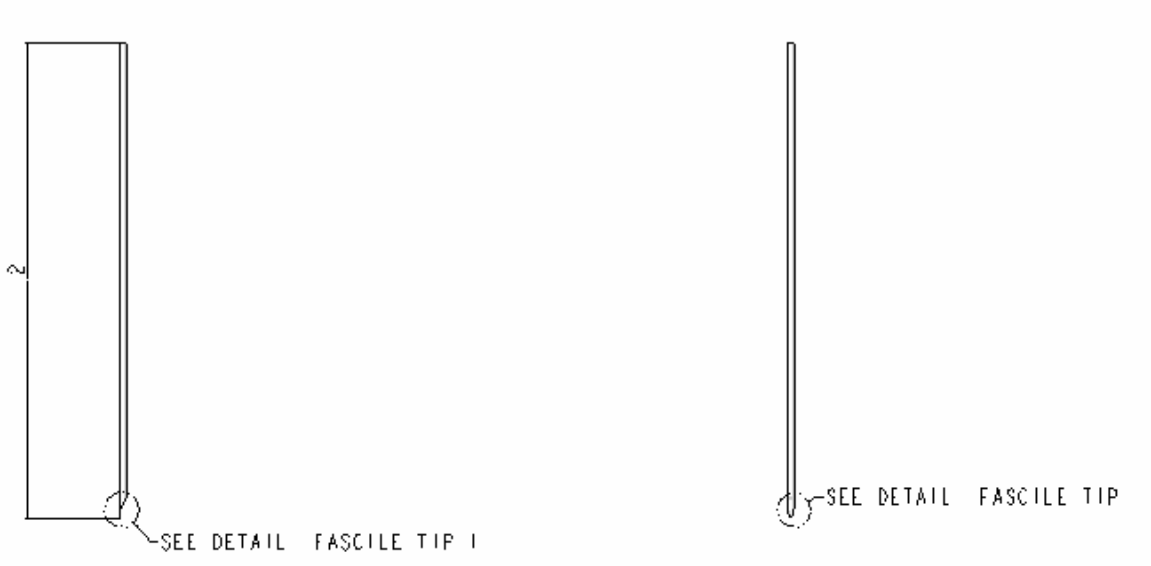

Figure 8:Schematic of the fascicle showing the dimensions in mm.

2.2 High speed video imaging of the mosquito feeding process

Numerous studies have been carried out to understand mosquito feeding process from a biological point of view. Our concentration however is to understand mechanics involved in this intricate process and as mentioned before find an explanation to how a fascicle which is so small in size doesn't fail due to high compressive axial loads it encounters while penetrating human skin. For this reason, a high speed video was taken of the feeding process to mainly capture the skin penetration by the fascicle and observe any behavior by the mosquito to compensate for mechanical buckling failure of the fascicle.

2.2.1 Observation and initial conclusions

Initially, we concluded that the labium or the outer sheath which covers the fascicle plays a very important role in the dynamical stability of the fascicle. This was in accordance with all the initial work carried out in this field.

Thus it was initially observed and concluded that as soon as the mosquito settles on its host, there is a time period where it is constantly poking on the skin, possibly looking for a "soft spot" to penetrate. The fascicle is still in the labium with just its tip out. During this "poking process" the mosquito keeps applying sudden dynamic impulse loads by kicking up her legs. Due to this load and the resistance offered by the skin, the proboscis buckles but does not fail. It is clear from the still image that the fascicle exhibits mode 1 form of buckling. It was concluded at this point that the labium actually provides lateral support along the whole length of the fascicle. This is analogous to buckling of a beam on an elastic foundation. The critical load for this beam is proportional to the Young's modulus and moment of inertia of the beam and is inversely proportional to the reduced length of the beam. Since the labium is acting on the continuously on the whole length of the beam, this value of free length becomes very small and thus the critical load for the proboscis becomes high and doesn't fail due to buckling. A more rigorous analysis

of this mechanism is explained later.

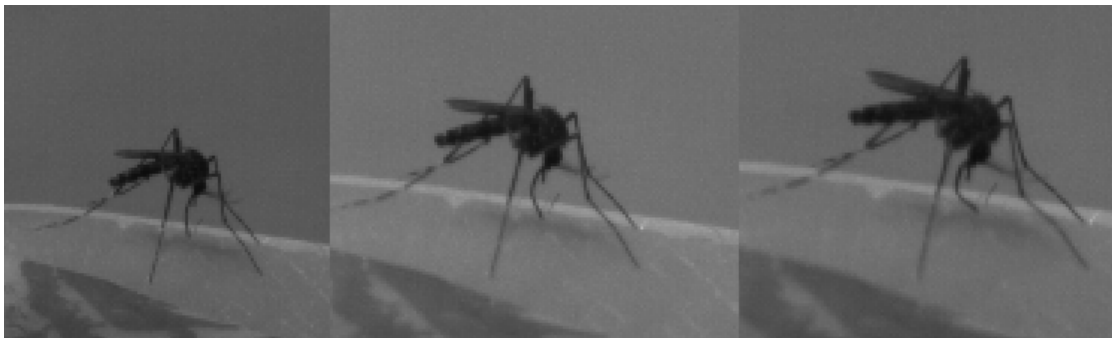

Figure 9:This still image shows the probing process during feeding.

The mosquito keeps applying impulsive loads to find a soft spot on the skin to penetrate. Clearly visible is the mode 1 form of buckling of the whole proboscis. It is apparent that at this stage no skin penetration has occurred so far. The radius of curvature is quite large, thus indicating a relatively high value of force being applied without failure**.**

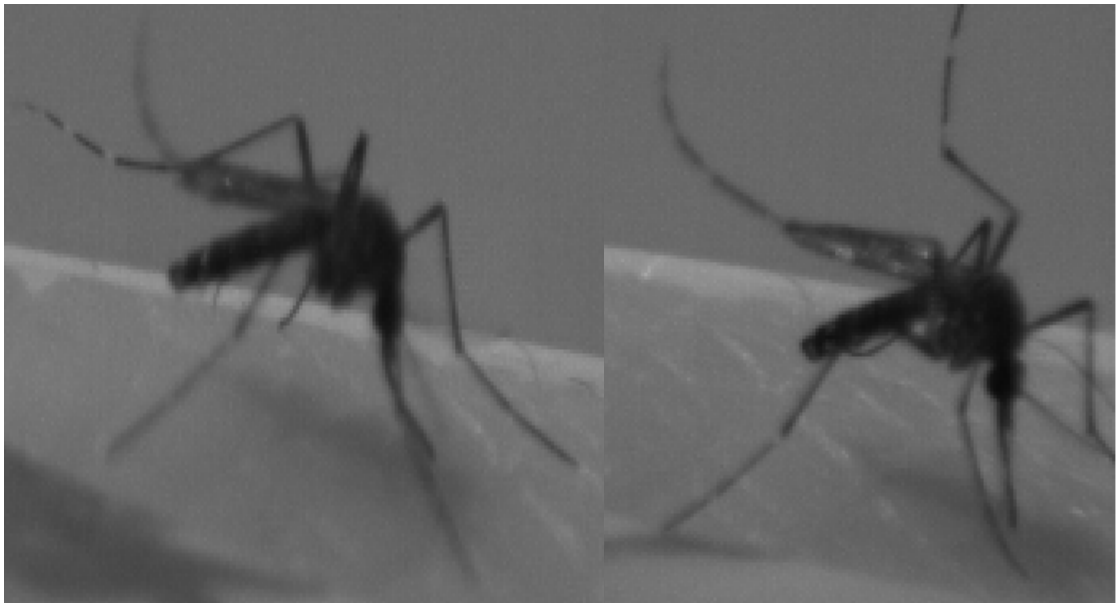

Figure 10: This image shows that the large impulsive force applied during the probing process is partly due to forward motion of the whole body applied by lifting and pushing of the legs

.

Once the critical load of the proboscis exceeds the failure load of the skin, penetration occurs. It is at this time that the risk of buckling failure is the maximum because resistance of the skin is maximum at its outer most layers. From a mechanics standpoint, once penetration occurs, the boundary condition for the fascicle changes from pinned to fixed at the end penetrating. New resistive forces come into play once a part of the fascicle is in the skin. There is a tangential shear force acting on the fascicle under the skin applied by the tissues which tries to resist further penetration. It is this tangential force which governs the downward movement. Once a part of the fascicle is under the skin, end shortening of the proboscis takes place. Due to this end shortening and the low stiffness of the labium, the labium starts folding at a rate proportional to the decrease of fascicle length above the skin. Thus, there are two factors involved in prevention of failure at this juncture. One, as the fascicle keeps penetrating further, there is a decrease in the free length of the fascicle above the skin resisting axial compressive load. Under the skin, it is probable that the compressive lateral force applied by the skin tends to reduce the effect of the shear force by the tissues. Thus with this reduction of free length, the critical force for buckling increases. The second factor initially proposed was that even though the fascicle folds up due to end shortening of the fascicle, it only folds up for a length proportional to the penetrated length. It still provides lateral elastic support for the difference in the original length and the new reduced length. This elastic support keeps changing dynamically as more and more of the fascicle penetrates.

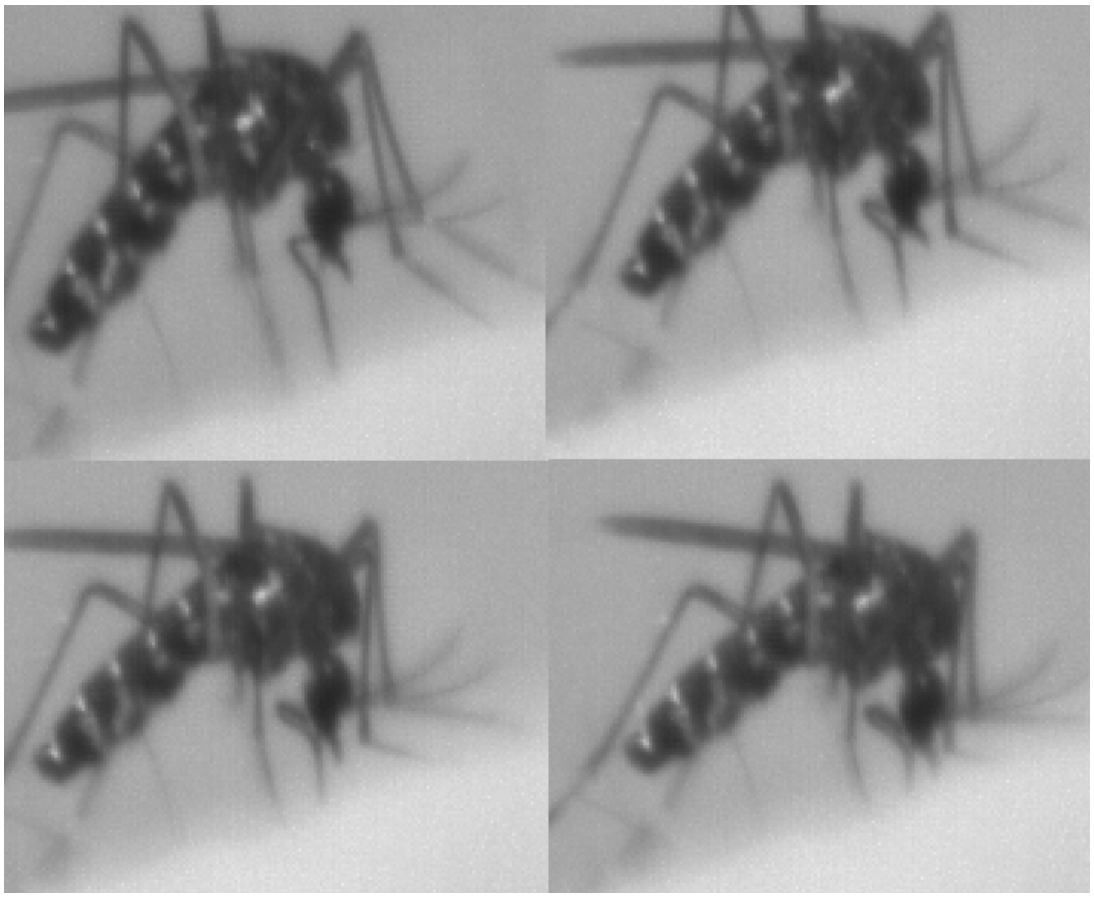

Figure 11: This still shows te process of skin penetration once soft spot in the skin has been und and initial penetration has occurred

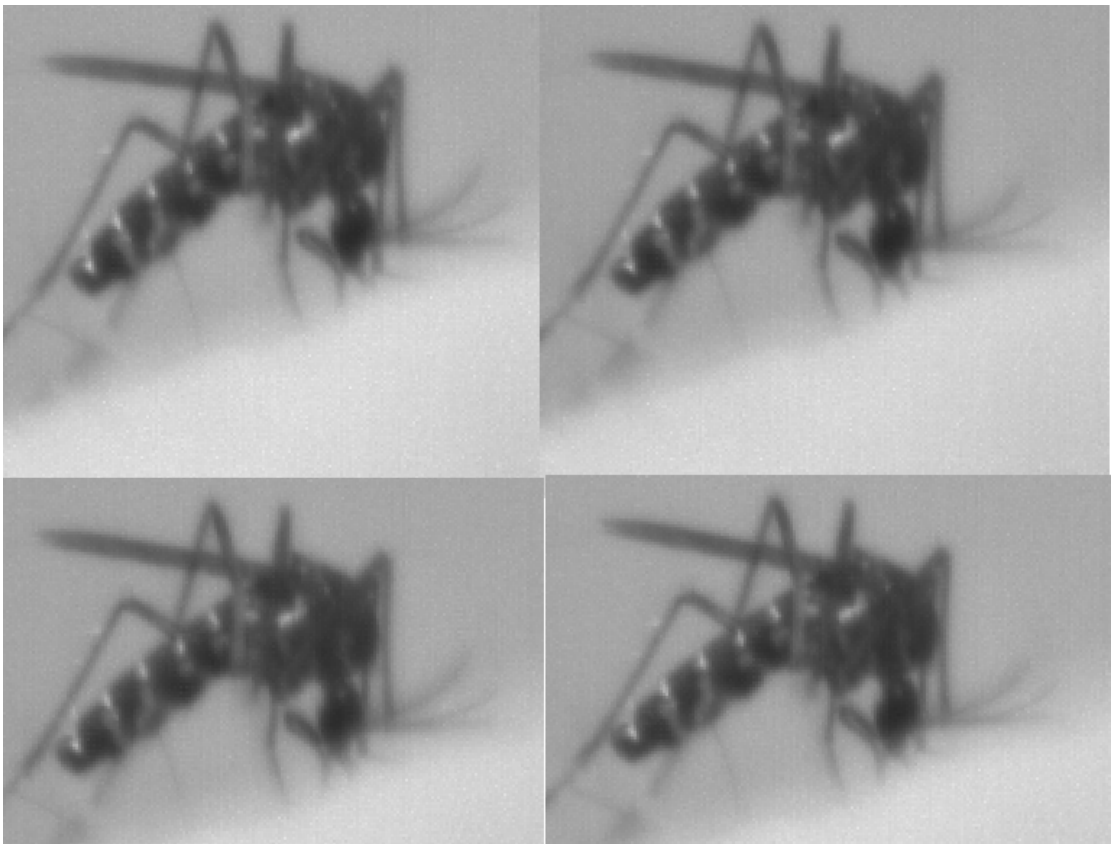

Figure 12: Still from the video showing kinking of the labium

The main reason to search for an alternate explanation was that it is clear that the labium has a stiffness which is many times lesser than the stiffness of the fascicle (as is clear from its folding). And even though it would have been extremely tough to come up with a way to measure the stiffness of the labium, it is clear that this explanation might not completely explain the stability mechanism of the fascicle.

2.3. Application of Non-Conservative force

One of the main observations from the high speed video was the constant movement of the mouth of the female mosquito (almost like a vibration). Initially thought of as

random, it was on further scrutiny noticed that there was a certain repetitiveness and non-randomness in this mouth movement. This movement and it's role in the stability of the fascicle is explained below.

Once the soft spot in the skin has been found, the mosquito applies an axial load which is equal to or higher than the failure load of the skin surface. However the magnitude of this load is also higher than the critical load for the fascicle because of which the fascicle begins to buckle and exhibits the mode 1 buckle shape due to the end condition being fixed at one end and being pinned at the other. At this juncture to compensate for the buckling, the mosquito moves her mouth (by the movement of the head) and keeps on applying a force in a direction not axial but at some angle to the fascicle (observed at around 75°-80° to the axial direction). This is the case of application of a non conservative force. The compressive force always acts in a direction of the tangent of the deflection curve. Thus at any point during the bending of the fascicle, the applied force can be resolved into two forces, one which acts in the lateral direction and one which acts in the axial direction. It is obvious that when the fascicle is in the straight configuration, there is only the axial component of the force acting. In the other configurations, i.e. when the fascicle is in a buckled form, although the net effect of axial force decreases due to change in the direction of the tangent, there is a lateral force which restores 'the fascicle back to its straight configuration. Thus the two components are making the fascicle penetrate further and also helping it return to its stable, straight configuration.

The above mentioned case of stabilization of beam with non-conservative forces/follower force acting on it can be solved by applying the dynamic theory of stability and explained in more detail later.

The maximum risk of failure for the fascicle is during the initial penetration stage. During this stage, the length of the fascicle is quite long and the resistance of the skin is at its highest. It is at this stage, maximum mouth movement was observed in the high speed video. Once the top most layer has been penetrated, there is an increase in the critical

force of the beam due to end shortening. There is also a decrease in the resistance offered by the skin and tissues with increase in depth of penetration.

In addition to this follower load stability mechanism, there is another stability mechanism which has been proposed which might play a role especially once the initial penetration has occurred. It has long been reported that a rope with bending stiffness, like a wire, can be stabilized at finite frequencies. It is often referred to as the 'Indian Rope Trick [15]. It has been proven that rapid, small amplitude; parametric harmonic excitation can balance a single pendulum in an upside down position. Similarly experiments have shown that this can be extended to wires and ropes where these harmonic excitations provide dynamical stability and prevent collapse of wires and ropes. This theory can also be extended to mosquito feeding where parametric vibrations of the mosquito's head provides further dynamical stability to the fascicle and prevents it from buckling.

Thus from the video, it seems to be clear that the reason why a fascicle which is only 30μm in diameter doesn't buckle due to the resistance offered by the skin is due to a multitude of stability phenomenon occurring. These stability theories should form the basic foundation for micro-needles, extremely small in size and therefore being painless and yet not breaking due to the skin resistive forces.

Chapter 3

Stability Mechanisms

3.1. Theory of elastic Foundation

As mentioned before, from the SEM images of the fascicle and the labium and after observing the high speed video of the feeding process, the initial hypothesis was that the labium or the outer sheath was providing lateral support to the fascicle, to prevent it from buckling. Further investigation was conducted to determine the stability of this system. The case mentioned above is analogous to the case of buckling of a bar on an elastic foundation [6]. According to this theory, if there are many equally spaced elastic supports of equal rigidity, their action on the buckled bar, can be replaced by the action of a continuous medium, the reaction of which, at each cross section of the bar, is proportional to the deflection at that cross section. An equivalent rigidity for the elastic medium can be expressed as

$$\beta = \alpha / a$$

where α is the spring constant of the individual support and a is the distance between the supports.

The energy method is used to calculate the critical value of the compressive force. The general expression is given by the series

$$y = a_1 \sin\frac{\pi x}{l} + a_2 \sin\frac{2\pi x}{l} + a_3 \sin\frac{3\pi x}{l} + \ldots$$

The strain energy of the bending member is

$$\Delta V_1 = \frac{EI}{2}\int_0^l \left(\frac{d^2 y}{dx^2}\right)^2 dx = \frac{\pi^4 EI}{4l^3}\sum_{n=1}^{n=\infty} n^4 a^2{}_n$$

lateral reaction of the elastic medium on an element dx of the bar is $\frac{\beta y^2}{2}dx$. Thus the total energy of deformation of the elastic medium is

$$\Delta V_2 = \frac{\beta}{2}\int_0^l y^2 dx$$

By substituting the series for y

$$\Delta V_2 = \frac{\beta l}{4}\sum_{n=1}^{n=\infty} a^2{}_n$$

The work done by compressive force P is

$$\Delta T = \frac{P\pi^2}{4l}\sum_{n=1}^{n=\infty} n^2 a_n^2$$

Equating the two, we get

$$\frac{\pi^4 EI}{4l^3}\sum_{n=1}^{n=\infty} n^4 a_n^2 + \frac{\beta l}{4}\sum_{n=1}^{n=\infty} a_n^2 = \frac{P\pi^2}{4l}\sum_{n=1}^{n=\infty} n^2 a_n^2$$

from which

$$P = \frac{\pi^2 EI}{l^2}\frac{\sum_{n=1}^{n=\infty} n^4 a_n^2 + \frac{\beta l^4}{\pi^4 EI}\sum_{n=1}^{n=\infty} a_n^2}{\sum_{n=1}^{n=\infty} n^2 a_n^2}$$

To find the critical value of P, it is necessary to find the relationship between the coefficients to make the above expression minimum. This is obtained by making all coefficients except one equal to zero to obtain a sine deflection curve. If am is the coefficient which is non zero, then

$$y = a_m \sin\frac{m\pi x}{l}$$

and

$$P = \frac{\pi^2 EI}{l^2}(m^2 + \frac{\beta l^4}{m^2\pi^4 EI})$$

When $\beta = 0$ there is no resisting medium and m=1 which is the case of simple buckling of a bar. If β is very small m is again equal to 1, thus for a very elastic medium the member buckles without any inflection point. By gradually increasing the value β we arrive at a condition where the expression is smaller for m=2 than for m=1. This indicates the situation when the inflection point is in the middle. The limiting value of the modulus β at which transition from m=1 to m=2 occurs is found from the condition that the value of P from the above equation should be the same irrespective of m=1 or m=2.

Thus

$$1 + \frac{\beta l^4}{\pi^4 EI} = 4 + \frac{\beta l^4}{4\pi^4 EI}$$

this implies that

$$\frac{\beta l^4}{4\pi^4 EI} = 4$$

Thus it is clear from the above equations that the critical load for a buckling case with an elastic foundation is higher than a simple buckling case. However this factor of increase is 4-6 depending on the number of half waves. In case of buckling observed in mosquito fascicle, this factor is 4 times. However this factor is not high enough to prevent the fascicle to penetrate the skin. Thus the theory of non-conservative force in which the factor is almost 20 was proposed for this case.

3.2 Theory of non-conservative force

As mentioned earlier, it has been observed that the mosquito is able to avoid buckling failure of the fascicle while penetrating the human skin by application of non-conservative forces. To understand this criterion, the classical problem of Beck's column was analytically solved. Beck's column consists of an elastic bar under the action of a tangential compressive force at it's free end, performing small oscillations about its

undisturbed form of equilibrium. The force is a follower in the sense that it always acts tangential to the curvature of the beam [16], [17].

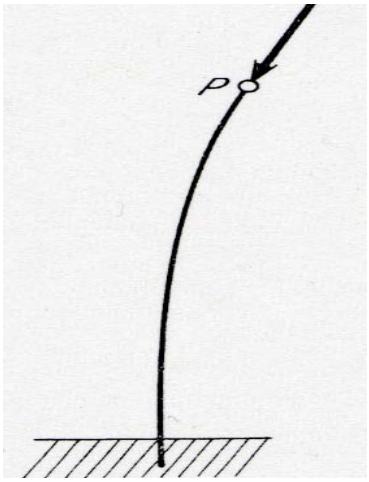

Figure 13: A beck's Column

Using the elementary theory of bending, the equation of small oscillations of the bar is of the form

$$EJ\frac{\partial^2 v}{\partial z^2} = P(f - v) - P\phi(1 - z) + L_j$$

where $v(z,t)$ is a small deflection at any point of the bar

$f(t)$ is the deflection at the free end

$\phi(t)$ is the angle of rotation of its end section

EJ is the bending stiffness of its section

L_j is the bending moment produced by the action of inertia forces.

By differentiating this equation twice and substituting

$$\frac{\partial^2 L_j}{\partial z^2} = \frac{-m\partial^2 v}{\partial t^2}$$

we get,

$$EJ\frac{\partial^4 v}{\partial z^4} + P\frac{\partial^2 v}{\partial z^2} + m\frac{\partial^2 v}{\partial t^2} = 0$$

The boundary conditions are fixed at one end and free at the other,

$$v(0,t) = \frac{\partial v(0,t)}{\partial z}$$

$$\frac{\partial^2 v(1,t)}{\partial z^2} = \frac{\partial^3 v(1,t)}{\partial z^3}$$

Equation 1 can be satisfied, if we set

$$v(z,t) = V(z)e^{i\Omega t}$$

where $V(z)$ is an unknown function and Ω is an unknown complex constant. Substituting this in the equation **1** we get the required 4th degree differential equation

$$\frac{\partial^4 V}{\partial \zeta^2} + \beta \frac{\partial^4 v}{\partial \zeta^2} - \omega^2 V = 0$$

where the non dimensional parameters are

$$\zeta = z/l, \ \beta = Pl^2/EI, \ \omega = \Omega l^2 (m/EJ)^{1/2}$$

The general solution of Equation 2 is of the form

$$V(\zeta) = C_1 \sin r_1\zeta + C_2 \cos r_1\zeta + C_3 \sinh r_2\zeta + C_4 \cosh r_2\zeta$$

Where

$$r_1^2 = \beta/2 + ((\beta/2)^2 + \omega^2)^{1/2}$$
$$r_2^2 = \beta/2 - ((\beta/2)^2 + \omega^2)^{1/2}$$

By using the boundary conditions, we can find the constants of integration:

$$C_2 + C_4 = 0$$
$$r_1 C_1 + r_2 C_3 = 0$$

$$C_1(r_1^2 \sin r_1 + r_1 r_2 \sinh r_2) + C_2(r_1^2 \cos r_1 + r_2^2 \cosh r_2) = 0$$

$$-C_1(r_1^3 \cos r_1 + r_1 r_2^2 \cosh r_2) + C_2(r_1^3 \sin r_1 - r_2^3 \sinh r_2) = 0$$

By equating the determinant to zero, we obtain the characteristic equation

$$\Delta(r_1, r_2) = r_1^4 + r_2^4 + r_1 r_2 (r_1^2 - r_2^2) \sin r_1 \sinh r_2 + 2r_1^2 r_2^2 \cos r_1 \cosh r_2 = 0$$

By replacing the non-dimensional parameters

$$\Delta(\omega, \beta) = \beta^2 + 2\omega^2 + \beta\omega \sin r_1 \sinh r_2 + 2\omega^2 \cos r_1 \cosh r_2 = 0$$

When there is no external force, $\beta = 0$ and roots of the equation are real, which correspond to the frequencies of natural oscillations of the unloaded bar. As the parameter beta increases the two smallest roots move closer and at some value of $\beta = \beta_*$, become multiple.

With further increase in the β the roots become complex. This value of β corresponds to the critical for P_{cr} and by finding the solution of the above equation we found the value of $\beta_* = 19.712$

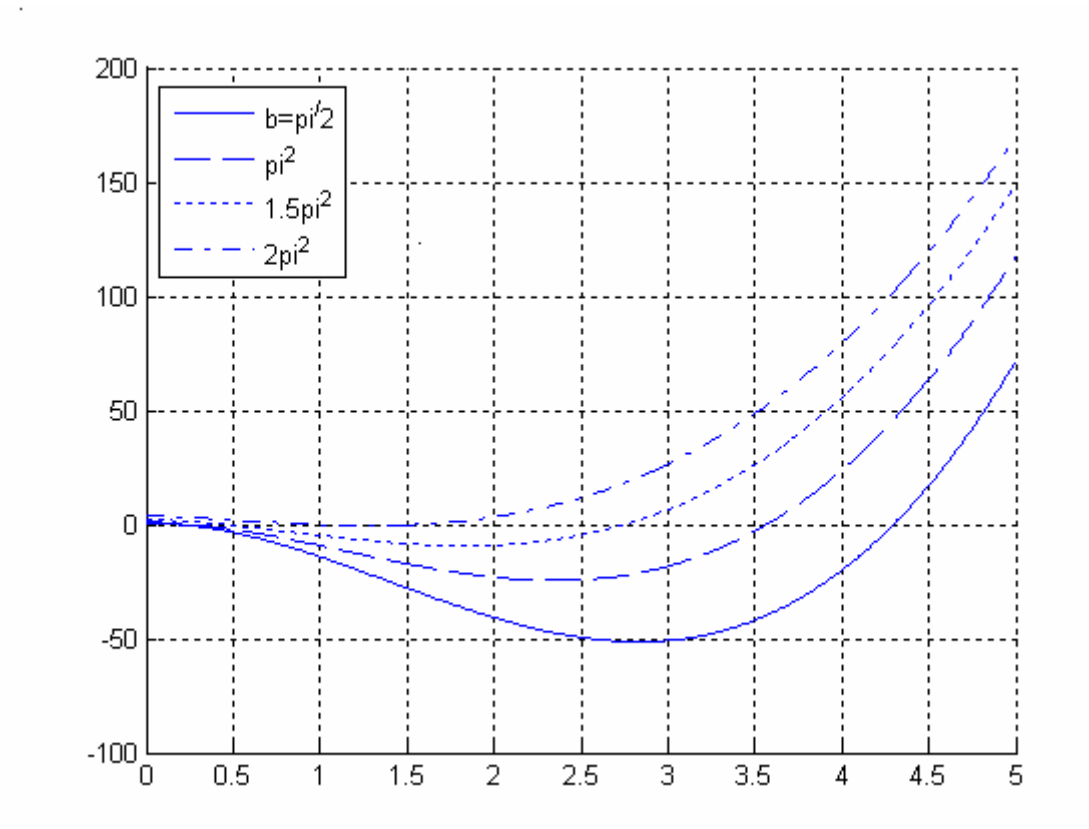

Figure 14: Plot of equation [3]

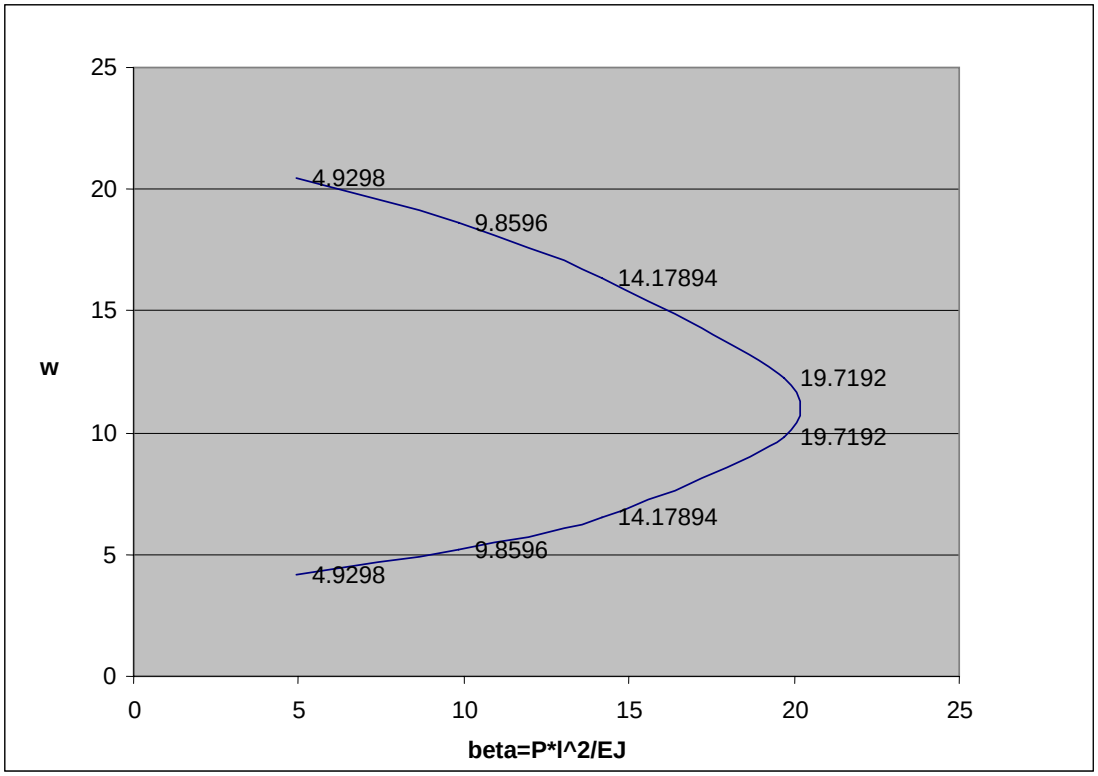

Figure 15: Solution to Beck's Column

$$P_{cr} = \beta * EJ / l^2$$

Thus clearly for the same end conditions, the critical buckling load of a column is much higher when the applied force is a follower force.

It has been observed and stated earlier, that from high speed video images it is clear that the mosquito keeps tilting its head to prevent it from buckling. The reason concluded is that by application of a non-conservative force, the fascicle is highly stable, and thus doesn't fail to compressive failure.

3.3. Methods of Application:

Aerodynamic and hydrodynamic loads, the force acting on parts of turbines and forces acting on turbines are in most cases non-conservative forces. However to induce the application of non-conservative forces on a particular structural member introduces a new

challenge. However, G Venkateshwara Rao et. al.[18] in their paper were able to use properly distributed piezoelectric actuators to apply and control varying magnitudes of follower forces on a cantilever beam to improve its stability. The follower force is applied through two piezoelectric layers, and the load applied by the piezoelectric layer to the column is of constant magnitude. The force exerted by the actuators is given by the equation

$$P_b = d_{31} E_p b V$$

Where

P_b is the magnitude of the follower load

d_{31} is the piezoelectric constant

E_p is the young's modulus for the piezoelectric material

b is the width of the piezoelectric cell

V is the applied voltage

Thus similarly, the stability of a needle which would buckle under normal axial loads can be improved which help to design smaller needles. It has been shown that the pain sensation during the skin penetration by a needle is dependant on the size of the needle. This mechanism shows a lot of potential in developing painless blood drawing device.

CHAPTER 4

Mechanical testing of Fascicle

4.1 Introduction

To characterize the skin penetration process by a mosquito, it is absolutely essential to determine the mechanical characteristics of the fascicle. However it was found that no such study existed which characterized the mechanical properties of the fascicle.

Conventional techniques are unable to test specimens from sum-millimeter sized regions. LaVan and Sharpe [19] tested small scale tensile specimens of a metal weldment. However due to higher relative strength and larger size of their samples, they were able to chose a bow-tie-shaped specimen which needed no gluing or clamping. In the case of a fascicle, the size limits this technique. Kompella and Lambros [20.] while characterizing the properties of cellulose fibers, made a small groove of 200 μm on the grips. These served as a cradle for the fiber ends. Once the fiber was set in place, a pipette was used to lay one drop of glue on each end of the fiber.

4.2 Experimental protocol

4.2.1 Sample Preparation

Mosquito fascicle was dissected from female Ae. Aegypti species. Sample handling imposed a major challenge as the characteristics of the fascicle are dependant on its moisture level. Due to this dependence, it was absolutely essential to glue the sample immediately and use micro droplets of water to constantly wet the sample during the glue

drying and testing process. Failure in doing so resulted in degradation of the sample and loss of any mechanical stiffness of the fascicle. This also restricted the number of samples that could be prepared at one time as the waiting period between two successive test runs increased the possibility of fascicle degradation. As mentioned before, a major problem encountered in the tensile testing of small fibers is the gripping arrangement. Gripping of the sample directly to the metal grips of the tester will result in its failure due to the force exerted by the grip on the fascicle. For this reason a paper strip former was used. The former was a strip of paper with dimensions 500mm by 12mm in which a very small hole of 0.6 mm diameter was punched. A 23 gauge syringe needle was used to punch this hole. The hole was punched with the help of a high resolution optical microscope to ensure exact circular profile. Care was also taken to remove any paper fiber lying across this hole as these fibers would affect the readings of the tester. Once the former was prepared and the fascicle isolated from the mosquito, using the high resolution microscope, the fascicle was laid carefully across the hole punched on the former. The location of the fiber across the hole is absolutely essential as any misalignment can create large bending strains in the sample. It has been assumed that there is no misalignment of the fascicle in this study. Once the fascicle was carefully placed and aligned on the strip of paper, adhesive drops was placed on each end of the fascicle. These drops were applied with a fine 23 gauge needles. The requirements of the adhesive was that it needed to be quick drying, water resistant and of reasonably high viscosity to avoid its spread along the fascicle. For this reason, Black max gel (Loctite Corp. CT) was chosen. It also proved to be easy to apply in small micro drops. Quick drying resulted in maintaining the mechanical stiffness of the fascicle. The next step was

to cut small slits at the punched hole to ensure that the 2 ends of the former were only linked by the fascicle. The cutting of the end of the strip proved to be another challenging process as any stress exerted on the sample resulted in its breakage. After numerous attempts which included using an acid dipped precision knife, using 2 separated formers it was decided to cut a part of the slit before loading the sample on the tester. At this point, a fine V-notch was also made at the ends to ensure easy cutting of the remaining part once the fascicle was loaded. The figure below shows the various stages of the sample preparation.

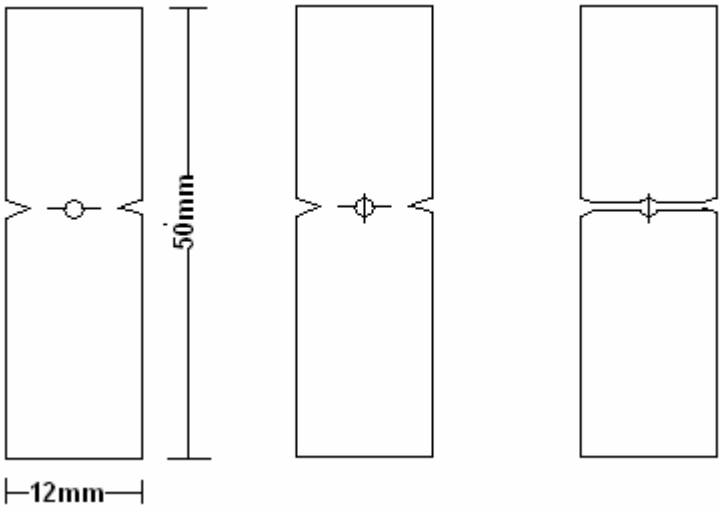

Figure 16: Sample Loading on a Paper Strip

Once the glue was dry, the sample was loaded on the tensile tester.

4.3 Test Set up

The tensile test was carried out using a material testing machine (Enduratec ELF3200, Minneapolis, Mn) with a [number] load cell (Sensotec, Columbus,OH). Tests were carried out at a displacement rate of 25 mm/sec. The fascicle was kept moist by placing a drop of water from a syringe exactly over the top of the fascicle. Force data was collected at 250 Hz using a DAQ card (DAQ card-AI-16E-4, NI Co.) The DAQ card has a maximum sampling rate of 250 Ks/s and can have up to 16 single ended channels. The BNC connector box is a rack mountable adapter used for simplifying connections of analog, digital and trigger signals to the DAQ card.

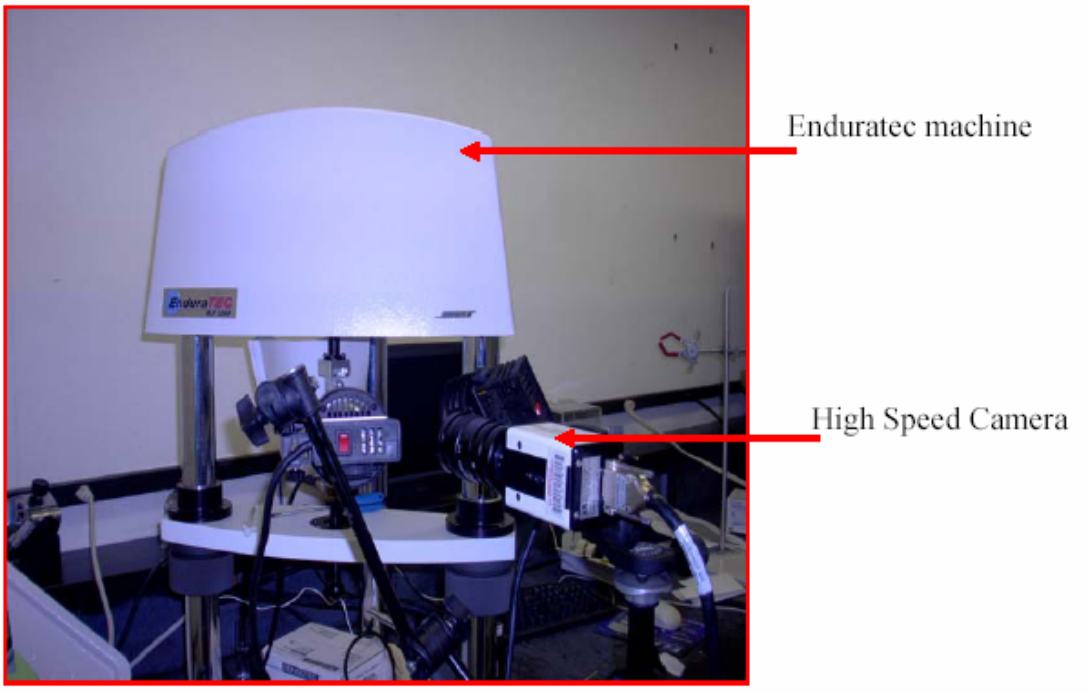

Figure 17: Enduratec Load Frame

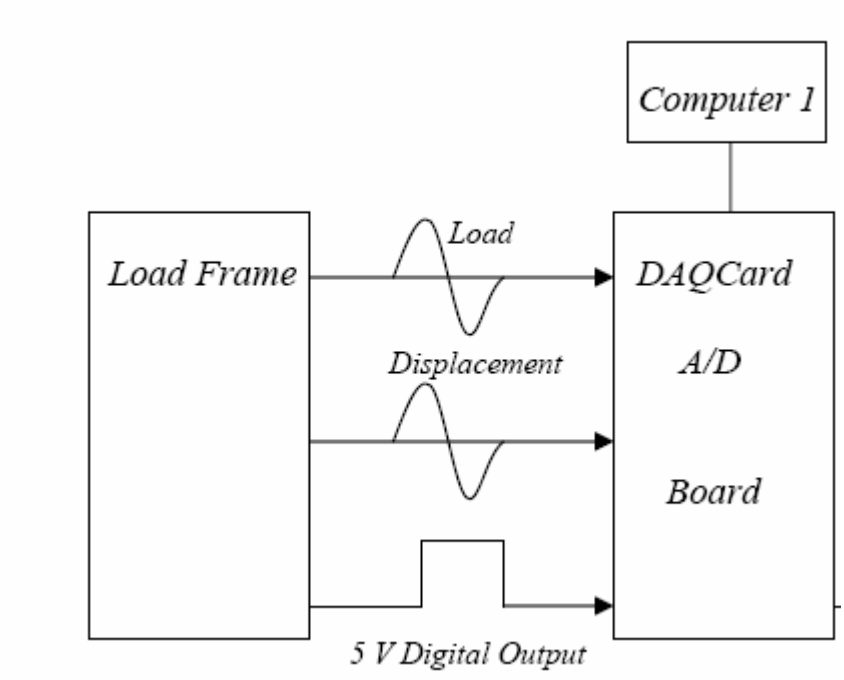

Figure 18: DAQ Set up

The clamps were initially positioned so that there was no slack in the sample, as it would not only give a little deviation in the readings but also since it was observed that the slack was damaging the fascicle. Once this whole set up was completed, the load was applied and load displacement readings obtained on the computer.

4.3.1 Challenges in Testing

In all 60 mosquito fascicles were dissected. Since the testing technique was being modified constantly, about 40 fascicles didn't make it to the testing stage and got damaged during the sample preparation stage itself. Initially it was not known that once the mosquito died, the fascicle needed to be removed and tested immediately as the fascicle would degenerate in a dead mosquito. The first 15 fascicles thus would fail at the

slightest touch of a forceps. For this reason it was decided to individually knock out the mosquitoes in the freezing chamber instead of doing them in batches. The choice of adhesive for gluing of the sample also proved to be a very decisive factor. Finally a resin based adhesive was chosen. Around 10 fascicles were lost during testing with various other adhesives. Some would need excessive drying time, while some had very low viscosity which resulted in the adhesive flowing along the length of the fascicle. But in the end the most challenging task was the cutting of the slits in the paper former. Since the actually cutting needs to be done once the sample has been loaded on the tester, the initial cut had to be made in such a way that the two ends of the paper strip didn't separate out completely. Once the sample was loaded on the tester and then cutting was attempted, due to the vertical loading, it was not possible to do much cutting without breaking the fascicle. During the cutting process, enough movement was being generated to damage the fascicle. Since the hole was of 0.6 mm diameter, cutting near the hole would result in damage of the fascicle. Several other techniques were also tested. It took 24 trials to finally come up with the suitable V-notch technique. Once the technique was perfected with other parts of the mosquito, the fascicle was stuck to the former and then it was cut to get the sample ready to load on to the tester. Once the sample was loaded, a very slight cut needed to be made to completely separate the paper strip ends from each other. In the end 5 tests were successfully conducted and for the first time experimental mechanical data for mosquito fascicle was obtained.

4.4 Results and Conclusions.

Stress Strain plots were obtained from the load displacement data obtained from the conducted tests. The specimen dimensions were approximated from SEM images of the fascicle and were used to calculate stress strain values. The cross sectional area of the fascicle was approximated at 0.000216 mm^2 and the initial gauge length at 2mm. As is clear from the plots shown below, fascicle shows non linear elastic behavior. In the next section, the theory of elasticity as applied to the Finite Element package ABAQUS is explained. By approximating the non-linear curve, the Young's modulus for the fascicle was found to be 420 MPa. In ABAQUS, even though the hyperelastic model was used, this value can be used for further investigating research on the fascicle, where linear isotropy is desired.

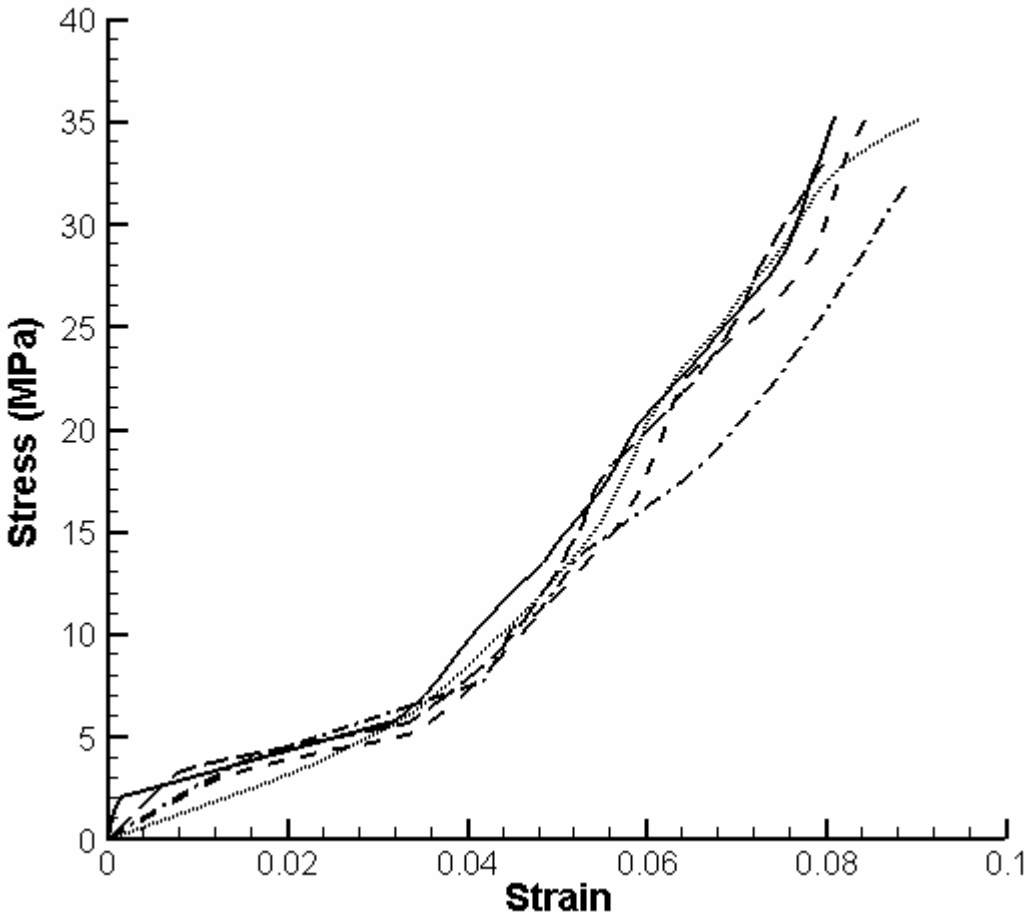

Figure 19: Stress Strain Curve for Fascicle

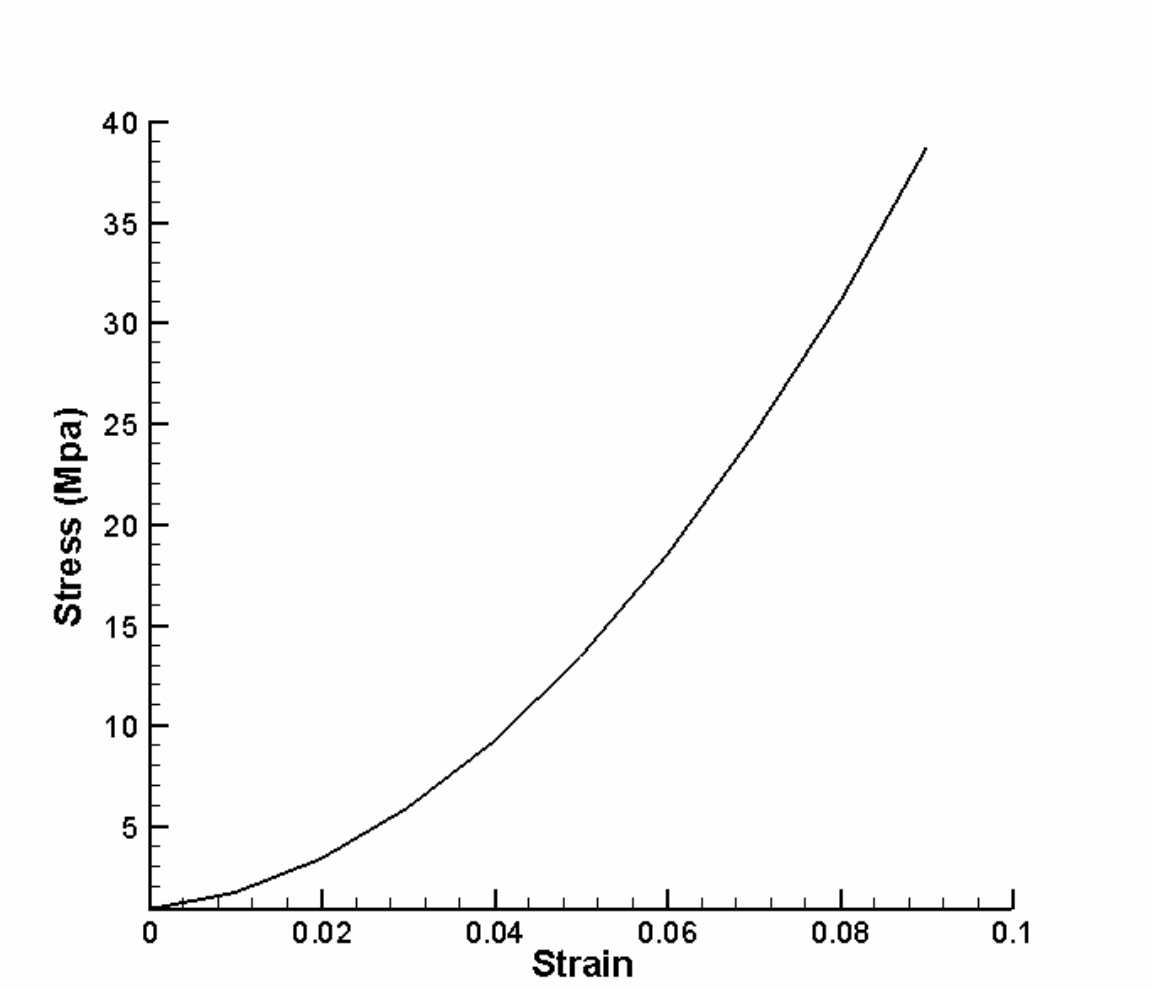

Figure 20: Hyperelastic curve fit for Fascicle Data

4.4.1 Theory of Hyperelasticity [21]

The most general type of nonlinear elastic behavior is the hyperelastic model. It is assumed that there is a strain energy density potential –U- from which the stresses are defined by

$$\sigma = \frac{\partial U}{\partial \varepsilon}$$

Where σ and ε are any work conjugate stress and strain measures. This form of elasticity model is generally used to model materials whose long-term response to large

deformation is fully recoverable. The constitutive behavior of a hyperelastic material is defined as a total stress-total strain relationship. Hyperelastic materials are described in terms of a "strain energy potential", U(ε) which defines the strain energy stored in the material per unit volume as a function of the strain at that point in the material. In ABAQUS there are several forms of strain energy potentials available to model approximately incompressible elastomers. When data from multiple experimental tests are available, the Ogden and Van der Waals forms are more accurate in fitting experimental results. When only one set of test data is available, the Marlow form is recommended. In this case a strain energy potential is constructed that will reproduce the test data exactly and that will have reasonable behavior in other deformation modes.

Since for the mosquito fascicle, only uniaxial tests were conducted, Marlow form of strain energy potential was used for Finite element modeling. The form of Marlow strain energy potential is

$$U = U_{dev}(\bar{I}_1) + U_{vol}(J_{el})$$

Where U is the strain energy per unit of reference volume, U_{dev} as its deviatoric part and U_{vol} as its volumetric part; $\bar{I}_1$ is the first deviatoric strain invariant defined as

$$\bar{I}_1 = \bar{\lambda}_1^2 + \bar{\lambda}_2^2 + \bar{\lambda}_3^2$$

where the deviatoric stretches $\bar{\lambda}_i = J^{-1/3}\lambda_i$, J is the total volume ratio; Jel is the elastic volume ratio and λi are the principal stretches. The deviatoric part of the potential is defined by providing the volumetric test data, defining the poisson's ratio, or specifying the lateral strains together with the uniaxial, equibiaxial or planar test data.

4.4.1.1 Uniaxial Tests

The uniaxial deformation mode is characterized in terms of principal stretches, λi, as

$$\lambda_1 = \lambda_U, \lambda_2 = \lambda_3 = 1/\sqrt{\lambda_U}$$

Where λ_U is the stretch in the loading direction.

The nominal strain is defined by

$$\varepsilon_U = \lambda_U - 1$$

From principal of virtual work, to get the nominal stress T_U

$$\delta U = T_U \delta \lambda_U,$$

$$T_U = \frac{\partial U}{\partial \lambda_U} = 2(1 - \lambda_U^{-3})(\lambda_U \frac{\partial U}{\partial \bar{I}_1} + \frac{\partial U}{\partial \bar{I}_2})$$

4.4.1.2 Smoothing the test data

There is always some corruption of experimental test data due to random noise. ABAQUS provides a smoothing technique to remove noise from the test data based on the Savitzky-Golay method. Each data point is replaced by a local average of its surrounding data points, so that the level of noise can be reduced without biasing the dominant trend of the test data. A cubic polynomial is fitted through each data point i and n data points to the immediate left and right of that point. A least-squares method is used to fit the polynomial through these 2n+1 points. The value of the data point i is then replaced by the value of the polynomial at the same position. Each polynomial is used to adjust one data point except near the end of the curve, where a polynomial is used to adjust multiple points. This process is applied repeatedly to all data points until two consecutive processes through the data produce nearly the same result.

Chapter 5
Finite Element Analysis

5.1. Introduction

Finite element simulations were used to study the parameters involved in the penetration of the human skin. ABAQUS 6.4 was used to carry out all simulations. There have been a few studies carried out to understand the mechanics of human skin penetration. Oliver A Shergold et al. [22] showed that the use of a hypodermic needle leads to the formation of a crack rather than a residual hole in the dermis. Davatzikos [23] used FEA to predict anatomical deformations of the human skin.

There have been a few experimental investigations on the forces involved in process of penetration by hypodermic needles. Kataoka et al. [24] conducted experiments to study the resistance forces acting on a needle. According to Kataoka, there are different forces acting on the needle including tip forces which act in the axial direction of the needle, frictional force acting on the sidewall of the needle shaft in the axial direction and a clamping force acting on the sidewall. The penetration force was found to be 1.1 N for the needle they used. The cross-section area of the needle was $0.05mm^2$. However it is easy to see that this value of penetration force will be directly dependent on the cross-section of the needle and smaller the cross-section, lower will be the value of this force. It is however important to understand these forces to understand the complexity of skin penetration.

For the study of the mechanics of blood drawing by a mosquito, scanning electron images were used to determine the size of the fascicle. Since the ultimate aim of the project is to explore the possibility of having a handheld blood drawing device, the simulations involved understanding the stresses and the forces involved for a needle with size similar to a fascicle and also explore ways to prevent the failure in the needle.

5.2. Skin Model

One of the first challenges involved in modeling the process of skin penetration is to model the human skin behavior, which would be fairly accurate and would give quick convergent solutions to the contact problem. Due to the complexity of skin behavior, the skin models have some order of inaccuracy in predicting their behavior. The skin consists of several distinct layer, each consisting of it's own components and structures. It behaves as a non-homogenous, anisotropic, non linear, visco-elastic material subjected to pre stress. Since it has been impossible to test the mechanical characteristics of individual layers of the skin in vivo, only data of the full skin is mostly available. There are a number of skin models which have been published but each model needed to be evaluated to be applied to a penetration problem for ease of convergence. J Z Wu et al.[25] assumed the skin to possess both nonlinear elastic and linear viscoelastic properties. The nonlinearly elastic properties are modeled as a hyperelastic material for which the Ogden strain function is used. The subcutaneous tissue is modeled as a sponge like porous material fully saturated with fluid. The poroelastic constitutive relation is based on the finite deformation theory with a deformation dependent hydraulic permeability due to the large deformation it undergoes. The complexity in this model arose from the poroelastic parameter, which takes a longer time to solve for and leads to certain convergence complications.

Oomens [26] and Hendricks [27] modeled the skin comprising of 3 layers, the top layer, the muscle layer and the fat layer. All 3 layers were modeled as hyperelastic materials and their properties were determined using data from Oomens et al.

Table 1: Skin Mechanical properties [26]

Skin layer	Thickness (mm)	ά	μ(MPa)
Skin	0.15	100	0.016
Muscle	1.1	30	0.012
Fat	1.25	5	0.02

Where ά is a temperature dependent constant used in the Ogden strain energy potential form. In this form the strain energy potential is given by the equation [21].

$$U = \sum \frac{2\mu_i}{\alpha_i}(\lambda_1^{\alpha_i} + \lambda_2^{\alpha_i} + \lambda_3^{\alpha_i} - 3) + \sum \frac{1}{D_i}(J^{-el} - 1)^{2i}$$

λ_i are the deviatoric principal stretches

α_i and μ_i are temperature dependant material parameters.

And the initial shear modulus

$$\mu_o = \sum \mu_i$$

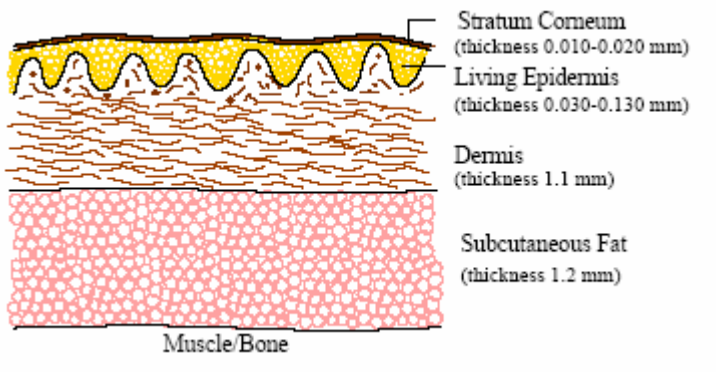

Figure 21: Layer of the skin [13]

The theoretrical pressure required to pierce the epidermis layer of the skin is 3.183 MPa [7]. However this pressure varies for with age and from person to person depending on the type of skin. As mentioned earlier the force exerted by the body is highly non-linear and varies with the cross sectional area of the needle. The skin in this study was modeled as a block with separate partitions representing the different layers of the skin. Individual sectional properties were assigned to each of the layers. Although the skin can be modeled as an infinite element, the fairly large section was taken for ease of convergence and simplification of modeling. It was found that the size of this section was big enough to avoid any effects of the boundary on the penetration zone. The skin model was placed on a rigid surface, which represents the bone. Since the stiffness of the bone is fairly high, it was modeled as a rigid surface. The contact between the rigid surface and the skin layer was assumed to have a very high coefficient of friction to prevent any sort of slipping between the skin and the rigid surface.

5.3. Contact Model

To estimate the parameters involved in the penetration of the human skin by a microneedle with dimensions similar to that of the fascicle, contact simulations were carried out. The fascicle was modeled as a 3D deformable homogenous part and meshed using an 8 node linear brick element with reduced integration controls. A pure master

slave relationship was used, with the needle being the master object. ABAQUS/Standard defines contact between two bodies in terms of two surfaces that may interact. The order in which the two surfaces are specified is critical because of the manner in which surface interactions are discretized. For each node of the first/slave surface, ABAQUS attempts to find the closest point on the second/master surface of the contact pair where the master surface's normal passes through the node of the slave surface. The interaction is then discretized between the point on the master surface and the slave node. The skin was meshed using 8 node brick elements, and the mesh density was made substantially higher at the top contact surface to get accurate results. The bottom part of the skin was supported by a rigid surface to mimic the skin-bone interaction. Small sliding formulation was used in this analysis. The formulation assumes that the surfaces may undergo arbitrarily large rotations but that a slave node will interact with the same local area of the master surface throughout the analysis. The slave node is constrained not to penetrate its own tangent plane on the master surface.

ABAQUS/standard uses Newton's method to solve the non-linear equilibrium equations. The solution is usually obtained as a series of increments, with iterations to obtain linear equilibrium within each increment. Increments must sometimes be kept small to ensure correct modeling of history dependent effects. Newton's method has a finite radius of convergence; too large an increment can prevent any solution from being obtained because the initial state is too far away from the equilibrium state that is being sought.

5.4. Element Formulation

In any contact based simulation, one of the most critical steps is to choose the right meshing elements. The accuracy of the analysis is contingent on the fact that right elements are used. In this case, due to the non-linearity of the skin behavior it was important that the proper elements were selected. During this learning curve, a number of important criterions were found that will not only be useful in further work but also demonstrates the element formulation in ABAQUS. It was found that first order triangular and tetrahedral elements should be avoided for stress analysis problems as

these elements are overly stiff and exhibit slow convergence with mesh refinement. Second order elements provide higher accuracy in ABAQUS/Standard than first order elements for problems that do not involve complex contact conditions, impact or severe element distortions. They are very effective in bending dominated problems. In ABAQUS/Standard, modified triangular and tetrahedral elements should be used in contact problems because the contact forces are consistent with the direction of contact. Similarly choosing reduced integration elements which uses a lower order of integration to form the stiffness matrix, reduces running time and cost. Thus fully integrated first order triangular and tetrahedral elements should only be used as filler elements in non-critical areas. Keeping these criterions in mind, element formulation in this analysis was carried out.

Initially for various material properties of the needle, a uniform axial displacement was given to the top node of the needle and the interaction was studied. As expected for low stiffness values, the fascicle would buckle due to high resistance forces. Thus the material properties of the needle were varied till the fascicle didn't buckle but was successful in skin compression. The resistant force value curve was obtained and the maximum resistant force at the contact nodes of the skin top surface was used to determine the force required for a needle with the dimensions of the needle to penetrate. The displacements were applied in 2 steps instead of 1 to ease convergence. It was observed that applying the total displacement to the top node of the needle in 1 step made the system diverge. Also for preliminary results, the needle was first modeled using a blunt end and then a sharp tip replaced the blunt end. The existence of sharp tips creates points with high stress concentrations and further cause divergence.

5.5. Results

To support the non-conservative theory applied to microneedles, the following procedure was adopted. Initially after setting up the geometry of the problem, the needle was assigned the properties of the fascicle which were found from the experimental tests

explained before. After setting the parameters and boundary conditions, only axial displacement was applied to the top of the needle. As predicted, the fascicle buckled without penetration since the stresses at the contact interface of the skin and the needle were not sufficient to break open the skin.

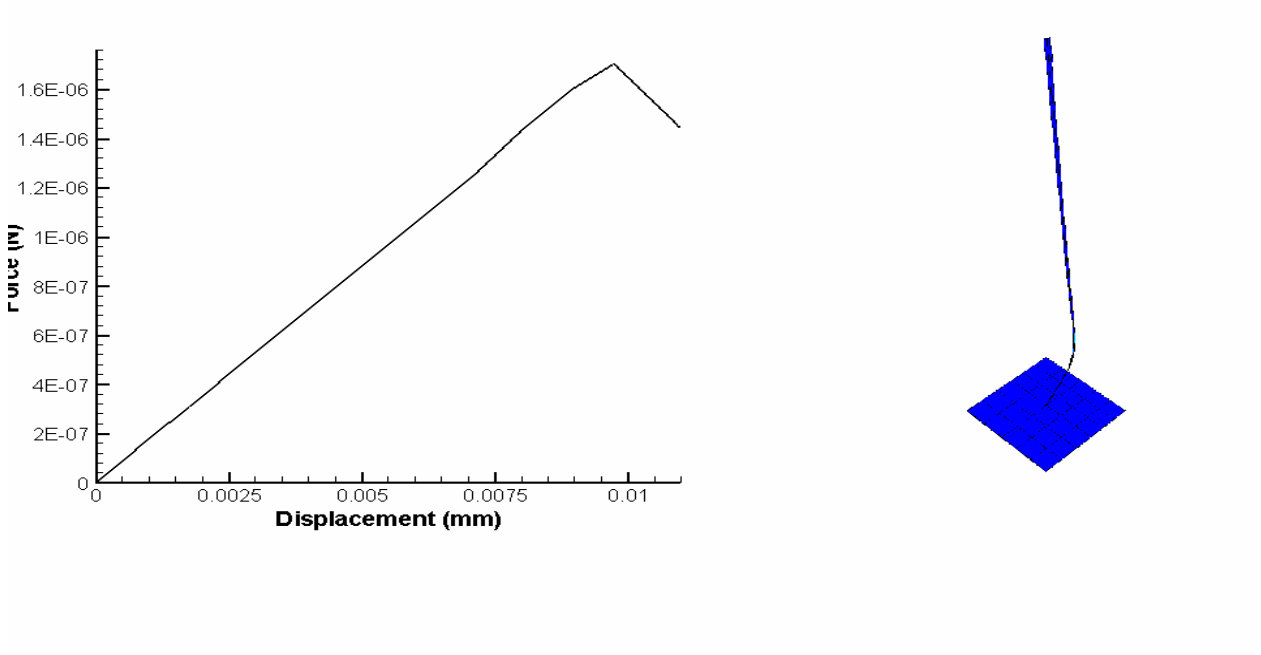

Figure 22: Buckling of the needle with application of axial displacement

The next step was to invoke the follower force algorithm in ABAQUS. The algorithm allows the applied force to follow the nodal rotation of the node at which it is applied. This is essentially the theory of non-conservative force where the applied force always acts tangential to the curvature of the member. A number of loads were applied, as, with low magnitude of follower force, the axial component was low enough that no penetration would occur. The parameter to decide whether penetration has occurred was the contact pressure on the interface of the needle and the skin. The obtained values were compared to the pressure at failure of skin obtained from literature and given earlier in the section. One of the main reasons for taking contact pressure as the factor to predict failure was because with penetration, the solution of the problem was diverging. A more rigorous method would be to use the adaptive meshing algorithm of ABAQUS. However in the present version, this is only supported in ABAQUS/Explicit. High pressure at the skin is accompanied by excessive mesh distortion. This distortion results in divergence of

the solution. Mesh refining reduces this divergence but cannot eliminate it. With adaptive meshing, the distorted meshes are constantly re-meshed to their initial state. The contact pressure method gives a faster and easier way to calculate failure. However, because of the nature of the problem and with non-linearity, there were some convergence issues, but less when compared to the other method.

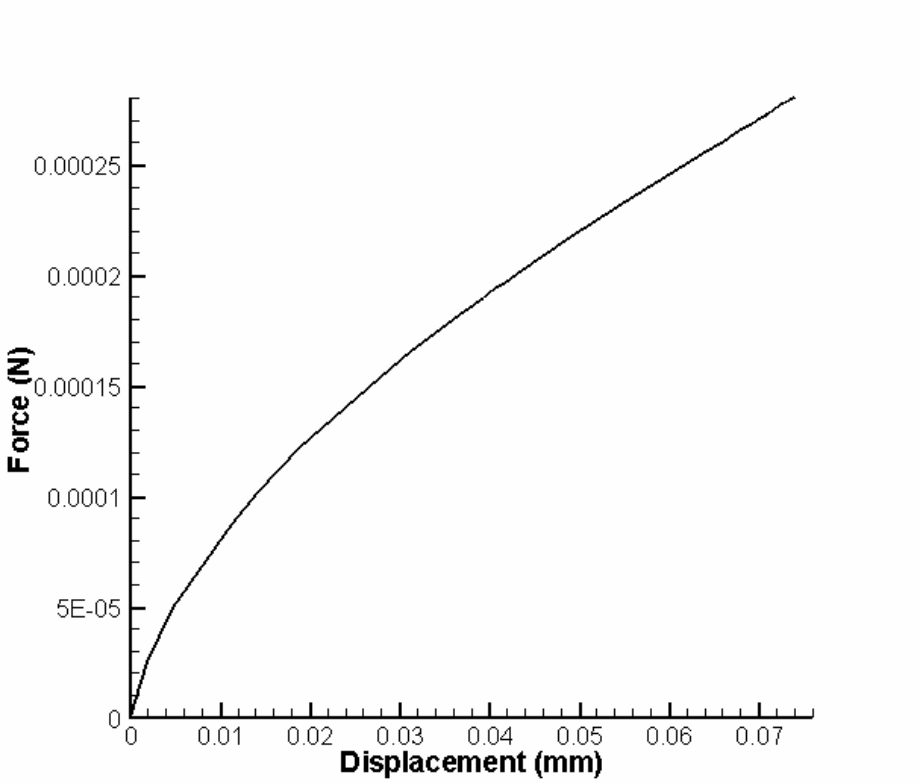

Figure 23: Load Displacement with 0.1N follower force

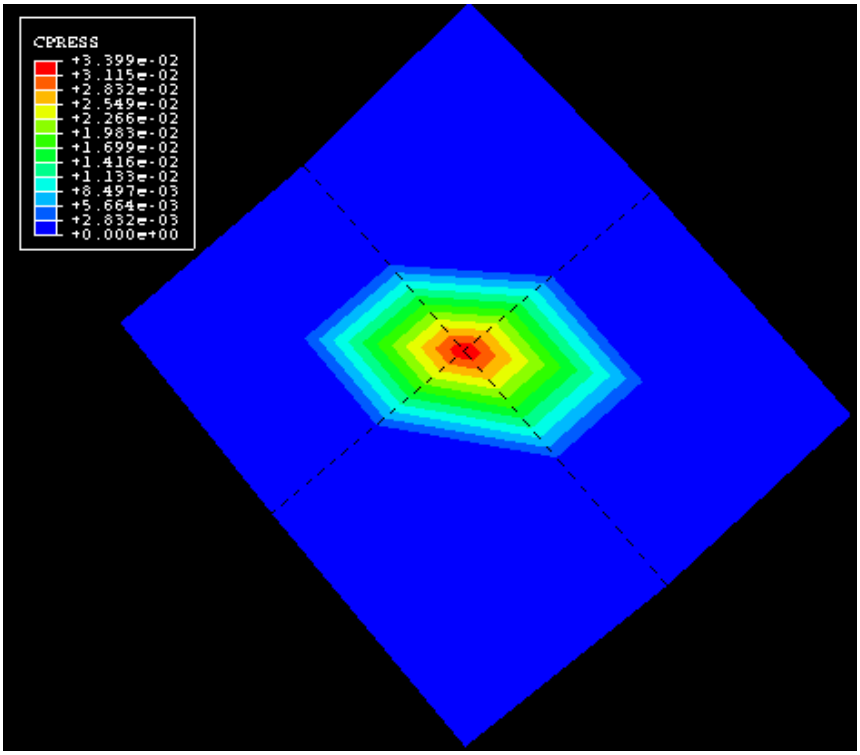

Figure 24: Contact Stress with 0.1N follower force

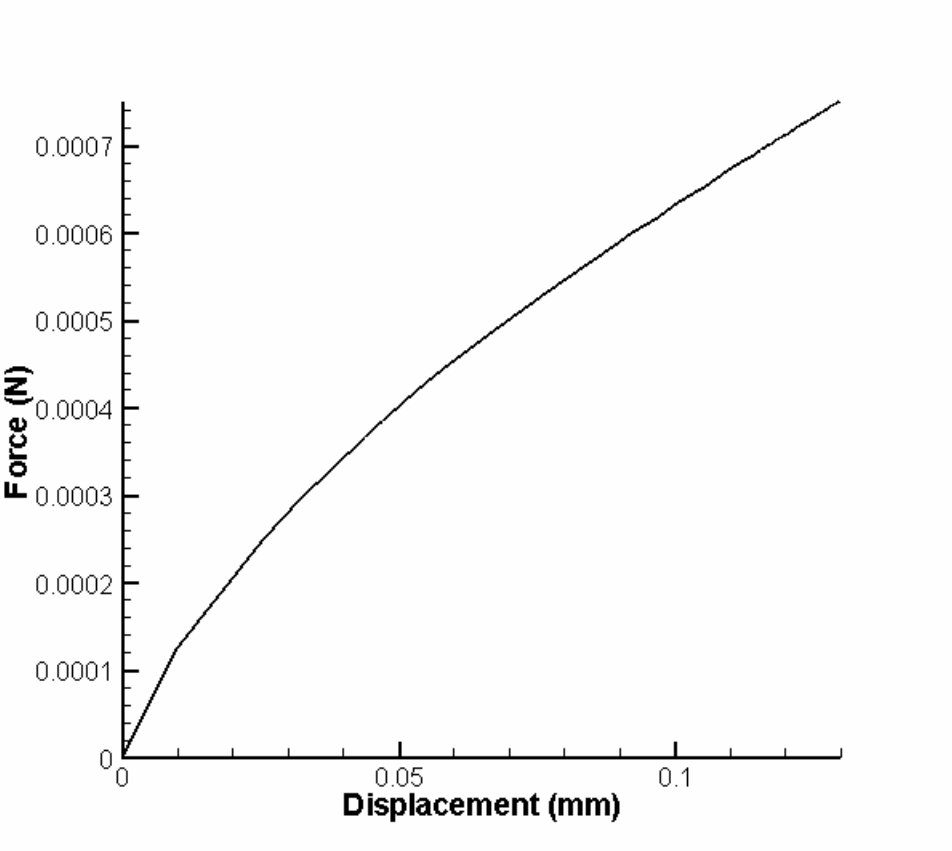

Figure 25: Load Displacement with 0.5N follower force

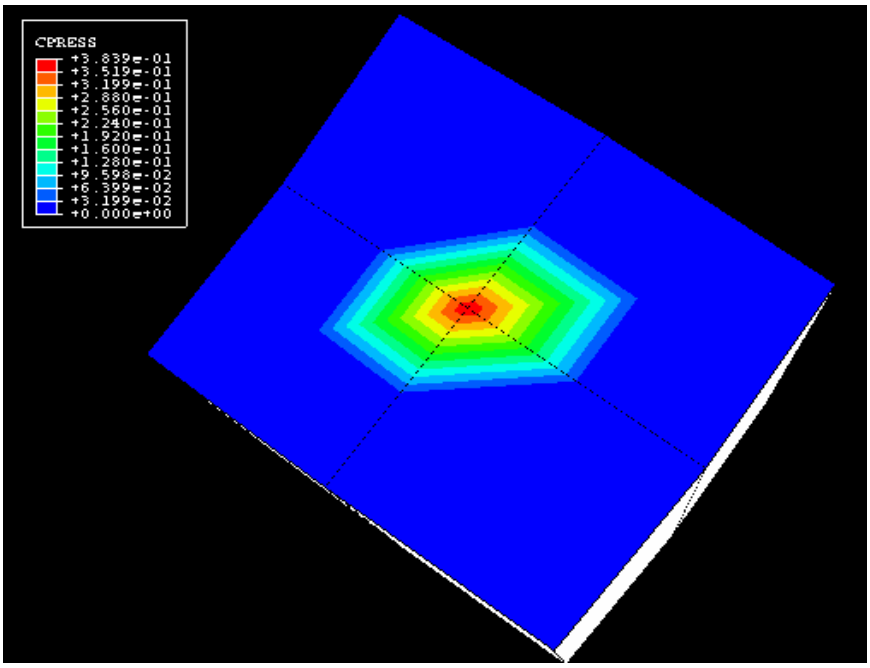

Figure 26: Contact Stress with 0.5N follower force

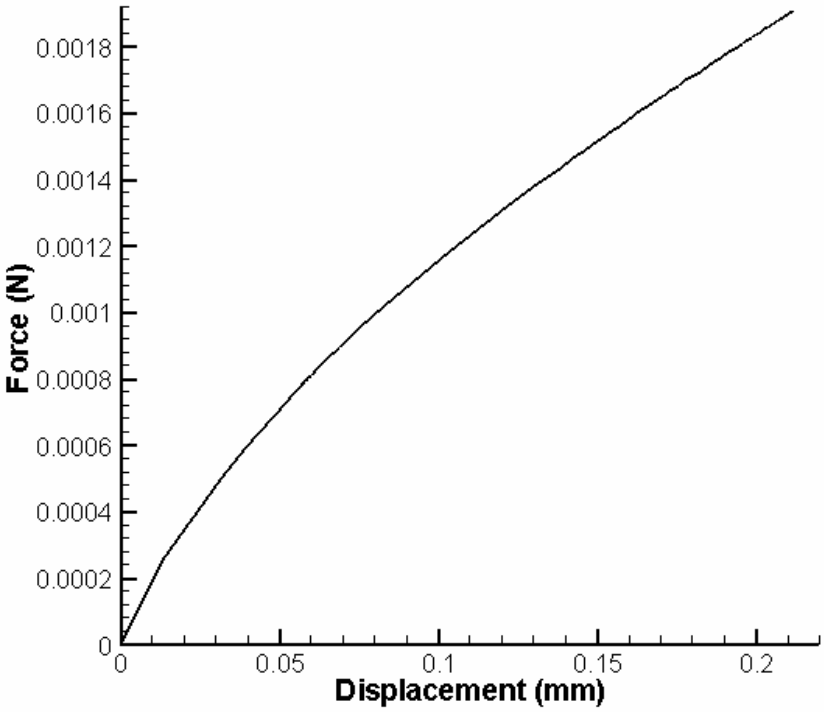

Figure 27: Load Displacement for 1N follower Force

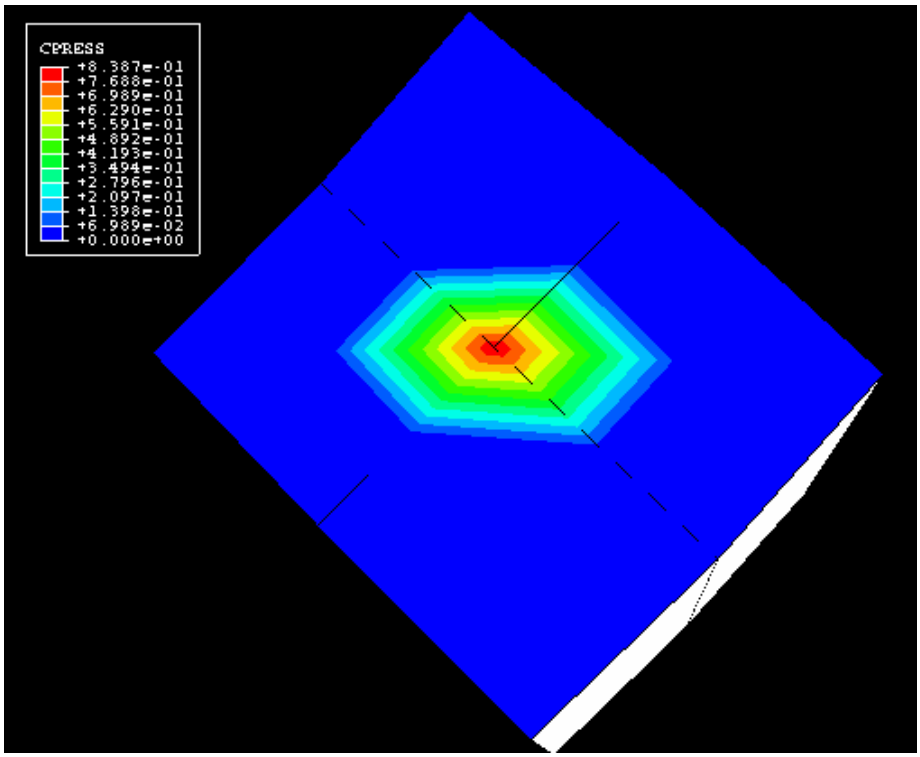

Figure 28: Contact Stress with 1N follower Force

The loads in the load-displacement curves indicates the net force acting in the axial direction. The horizontal component of the force prevents the needle from buckling. The contour plots show the stresses generated by the needle on the surface of the skin. As can be seen, this value of stress increases with increase in the value of the follower force. Although the simulations due to convergence issues are not able to predict for higher values of follower force, they are able to support the theory that with the application of a follower force, the stability of the needle increase.

Chapter 6

Conclusion:

The main object of this project was to understand the mechanics of buckling prevention in mosquitoes during blood feeding. To understand this, Scanning electron microscopy images of the mosquito fascicle were studied to understand the geometry of the fascicle. High-speed video of the feeding process gave an insight into various buckling modes observed in the fascicle and mosquito behavior to prevent failure. From these observations, a theory of stability was proposed which would increase the stability of any micro needle and prevent risk of failure. To further strengthen this concept Finite element Analysis was done to model the penetration of the human skin and show that the penetration of the fascicle into the skin would only be possible with the application of non-conservative load. To conduct these simulations, fascicle mechanical properties were determined using micro tensile testing of individual fascicles. This characterization of the fascicle according to our knowledge is the first such study which gives an insight into the mechanical properties of the fascicle. The simulations are able to show that with application of follower loads, the needle applies a much higher load on the skin for penetration, without buckling. It is thus concluded that at some value of follower force (about 2N) the fascicle is able to penetrate the skin without buckling. To get more accurate results and to get results for higher values of follower force, the meshing technique needs to be changed to adaptive meshing. This will be possible with a higher version of ABAQUS.

List of References

[1] Stoeber B, Liepmann D- Design, fabrication and testing of MEMS syringe

[2] Smart WH, Subramanian K- The use of silicon microfabrication technology in Painless blood glucose monitoring- Diabetes Technology and Therapeutics Vol.2, No.4 2000

[3] Wand PM, Cornwell M, Prausnitz MR- Minimally invasive extraction of dermal interstitial fluid for blood glucose monitoring- Diabetes Technology and Therapeutics Vol. 7 No.1 2005

[4] S. Kaushik, A.H. Hord, D D Denson, D V. McAllister, S Smitra, M G Allen and M G Prausnitz- "Lack of pain associated with microfabricated needles," Anesth. Analag. Vol.92, pp.502-5004,2001

[5] Giorgio E. Gattiker, Karan V. L S. Kaler and Martin P. Mintchev- Electronic mosquito: designing a semi invasive Microsystem for blood sampling, analysis and drug delivery applications. Microsyst. Technol (2005) 12, 44-52

[6] Timoshenko S – Theory of elastic stability- Mcgraw-Hill Book Company,Inc. First Edition.

[7] Jeffrey D. Zahn, Neil H. Talbot, Dorian Liepmann and Albert P. Pisano- Microfabricated Polysilicone microneedles for minimally invasive Biomedical Devices". Biomedical Microdevices 2:4,285-303,2000

[8] Rashad Sharaf, Priyanka Aggarwal, Karan V I S Kaler and Wael Badawy- "On the design of an electronic mosquito: Design and Analysis of the Microneedle".Proceedings of the International Conference on MEMS, NANO and Smart systems (ICMENS'03)2003.

[9] Han J G E Gardeniers, Regina Luttge, Erwin J W Berenschot, Meint J. De Boer et al.- " Silicon Micromachined Hollow Microneedles for Transdermal Liquid Transport". Journal of Microelectromechanical systems, Vol. 12, No.6,2003.

[10] A N Clements- "The biology of Mosquitoes"-Volume 1 Chapman and Hall

[11] Harbach, R E and Knight K.L.-"Taxonomists glossary of Mosquito Anatomy".- Plexus Publishing Inc. New Jersey (1980)

[12] Owen W. B.-"Morphology of the head skeleton and muscles in the mosquito", Culiseta inornata (Williston)- J. Morphol,1983,51-85

[13] Vogel R. –" Kritische und erganzende Mitteilungen zur Anatomie des Stechsapparats der Culiciden und Tabaniden". Zool Jb. 42, 259-82 1921

[14] Mellink J.J and van den Bovenkamp-" Functional aspects of mosquito salivation in blood feeding of Aedes aegypti. Mosq. News, 41, 115-119 (1981)

[15] Champneys AR, Fraser WB- "The Indian Rope Trick for a parametrically excited flexible rod linearized analysis"- Proceedings of the royal society of London A,2000.

[16] V V Bolotin- Nonconservative Problems of the Theory of Elastic Stability (A Pergamom Press Book)

[17] Beck, M- Die knicklast des einseitig eingespannten tangential gedruckten Stabes. Z angew. Math. Phys.3 (1952)

[18] G Venkateshwara Rao, Gajbir Singh – A smart structures concept for the buckling load enhancement of columns. Smart. Mater. Struct. 10 (2001)

[19] D. A La Van, W N Sharpe Jr. Tensile Testing of microsamples, Exp. Mech. 39 (3) (1999) 210-216

[20] Kompella M K, Lambros J-“ Micromechanical characterization of cellulose fibers”. Polymer Testing 21 (2002) 523-530

[21] HKS ABAQUS Theory manual (ver.6.4) Pawtucket (USA); Hibbitt, Karlsson and Sorensen Inc

[22] Oliver Shergold, Norman A Fleck- Mechanism of deep penetration of soft solids- ASME journal of Biomechanical engineering, 2004

[23] Davatzikos, Shen, Mohammed, Kyriacou- A framework for predictive modeling of Anatomical Deformations, IEEE Transactions of medical imaging, Vol.20,No. 8,Aug2001

[24] Kataoka H, Washio T et al. – Measurement of the tip and Friction force Acting on a needle during penetration, Medical Image Computing and Computer-Assisted Intervention - MICCAI 2002: 5th International Conference, Tokyo, Japan, September 25-28, 2002, Proceedings, Part I.

[25] Wu JZ, Dong RG, Rakheja S et al.- A structural fingertip model for simulating of the biomechanics of tactile sensation- Medical engineering and Physics 26 (2004) 165-175

[26] C W J Oomens, O F J T Bressers, E M H Bosboom, C V C Bouten : Deformation Analysis of supported buttock contact. BED-Vol 50, 2001 Bioengineering Conf ASME

[27] Hendriks F M et al. Mechanical Properties of different layers of the skin http://www.bmt.tue.nl/pdf/postersonderzoekdag2001/fhendriks.pdf